Journal of Computational Mathematics
Vol.xx, No.x, 2025, 1–33.

http://www.global-sci.org/jcm
doi:10.4208/jcm.2504-m2024-0211

SPECTRAL SOLUTIONS OF A FRACTIONAL-ORDER MATHEMATICAL MODEL FOR LUNG CANCER, SENSITIVITY ANALYSIS, AND FEEDBACK CONTROL*

Khadijeh Sadri[1)] and David Amilo
Mathematics Research Center, Near East University TRNC, Mersin 10, Nicosia 99138, Turkey;
Department of Mathematics, Near East University TRNC, Mersin 10, Nicosia 99138, Turkey;
Emails: khadijeh.sadrikhatouni@neu.edu.tr, amilodavid.ikechukwu@neu.edu.tr
Evren Hincal
Mathematics Research Center, Near East University TRNC, Mersin 10, Nicosia 99138, Turkey;
Department of Mathematics, Near East University TRNC, Mersin 10, Nicosia 99138, Turkey;
Research Center of Applied Mathematics, Khazar University, Baku, Azerbaijan
Email: evren.hincal@neu.edu.tr

Abstract

A fractional-order mathematical model of lung cancer is used to describe the dynamics of tumor growth and the interactions between cancer cells and immune cells. To obtain approximate solutions and better understand the behavior of the state functions, a pseudo-operational collocation scheme employing shifted Jacobi polynomials as basis functions is introduced. Initially, the existence and uniqueness of solutions to the model are established using the Leray-Schauder fixed-point theorem. Error bounds for the residual functions are estimated within a Jacobi-weighted L^2-space. To enhance the accuracy and reliability of the results, two distinct strategies are implemented: sensitivity analysis and feedback control. The feedback control of the proposed pseudo-operational spectral method is performed using the method of Lagrange multipliers, marking its first application in this context. Spectral solutions are derived by applying the pseudo-operational scheme to both the original model and the model with control functions. Improved performance and outputs are anticipated following the application of the feedback control strategy. Finally, comprehensive biological interpretations of the results are provided, offering insights into the practical implications of the model.

Mathematics subject classification: 65K05, 93A30, 92B05, 37M05.
Key words: Fractional-order model of lung cancer, Fractional operators, Existence and uniqueness, Jacobi collocation method, Feedback control strategy.

1. Introduction

Fractional calculus is the generalization of the classical integer-order calculus. Fractional operators possess memory effects that integer-order integral and derivative operators are not able to represent them. These operators are especially applicable in modeling systems that emerged in physics, chemistry, biology, environmental data, and so on. Since fractional operators are non-local, they take notice of the entire history of a phenomenon rather than its current behavior. Indeed, fractional calculus provides deeper intuitions and more precise models [3, 15, 30, 39].

* Received September 26, 2024 / Revised version received January 18, 2025 / Accepted April 3, 2025 / Published online June 4, 2025 /
1) Corresponding author

Mathematical modeling of diverse diseases helps researchers to understand how diseases can spread through the body or population. They furnish insights into figuring out the mechanisms, dynamics, transmission ways, and factors influencing the propagation of diseases. Mathematical models can simulate the effect of diverse interferences, for instance, vaccination, quarantine, and social distances on disease transmission. Therefore, researchers and healthcare professionals can predict the future treatment of the disease and evaluate various strategies to control it [4, 5, 7, 10, 11, 18, 36]. Among different types of cancers, the study of causes, mechanisms, and therapy strategies of lung cancer is vital for its high mortality rate. That is why, researchers have simulated various models to describe the growth of lung cancer in lung tissues [1,6,13,31,42,46,49]. From the point of view of the numerical solution, Amilo *et al.* [4] solved numerically their suggested model of progression of the lung cancer using an Adams-Bashforth predictor-corrector method. Authors in [38] presented a fractional model of tumor-immune system interaction related to lung cancer and applied an Adams-type predictor-corrector method to estimate numerical solutions to the proposed model. Hassani *et al.* [21], used the generalized Laguerre polynomial method to obtain optimal solutions of a model of lung cancer.

Spectral methods, including the Galerkin, tau, and collocation, are a class of techniques utilized to solve different functional equations where the solution to the given problem is represented as a linear combination of basis functions [14, 26, 27, 29, 35, 50]. Basis functions can be eigenvalues of some second-order differential equations such as Jacobi, Laguerre, and Hermite polynomials [2, 12, 16, 23, 24, 43, 45, 47, 48, 51]. Orthogonal Jacobi polynomials play a significant role in different areas of mathematics and its applications. These polynomials are employed in various numerical techniques to approximate and interpolate unknown functions in given functional equations. Jacobi polynomials include two parameters $\theta, \vartheta > -1$ which by varying values of θ and ϑ, different special cases of these polynomials appear (for instance, Legendre polynomials for $\theta = \vartheta = 0$, Chebyshev polynomials of the first and second kinds for $\theta = \vartheta = -0.5$ and $\theta = \vartheta = 0.5$, respectively). In this way, the effect of varying two parameters on approximate solutions can be investigated. The trace of Jacobi polynomials can be seen in many research works as basis functions. For instance, to solve fractional integro-differential equations [12, 27, 35, 45, 47, 50] and time- or time-space fractional partial differential equations (PDEs) including the pantograph PDEs, Fisher-Kolmogorov equation, diffusion-wave equations, hyperbolic PDEs, telegraph equations, distributed-order fractional Schrodinger equation and so on [17, 22–24, 33, 48].

As we know, Jacobi polynomials have not been used to numerically solve systems of fractional differential equations obtained from mathematical modeling of diseases. For this reason, this research deals with applications of these polynomials for such models. A fractional-order system of differential equations, presented in [4], reveals the interactions between cancer cells and immune cells in lung tissues and cancer cells that have spread to other parts of the body as follows:

$$\begin{cases} {}_0^C\mathcal{D}_\tau^\zeta \mathcal{N}(\tau) = \lambda \mathcal{N}(\tau)\left(1 - \dfrac{\mathcal{N}(\tau)}{\kappa}\right) - \mu \mathcal{N}(\tau)\mathcal{P}(\tau) - \beta_1 \mathcal{N}(\tau)\mathcal{I}(\tau), \\ {}_0^C\mathcal{D}_\tau^\zeta \mathcal{I}(\tau) = \varphi_1 \mathcal{I}_0 + \varphi_2 \mathcal{N}^2(\tau) - \varphi_3\, \mathcal{I}(\tau) - \beta_2 \mathcal{I}(\tau)\mathcal{P}(\tau), \\ {}_0^C\mathcal{D}_\tau^\zeta \mathcal{P}(\tau) = \gamma \mathcal{N}(\tau)\, \mathcal{P}(\tau) - \delta \mathcal{P}(\tau) - \beta_3\, \mathcal{I}(\tau)\mathcal{P}(\tau), \end{cases} \tag{1.1}$$

where $\mathcal{N}(\tau)$ represents the number of cancer cells in lung tissues at time $\tau, \mathcal{I}(\tau)$ represents the number of immune cells in lung tissues at time τ, and $\mathcal{P}(\tau)$ represents the number of cancer cells that have spread to other parts of the body at time τ, $\tau \in [0, T]$. ${}_0^C\mathcal{D}_\tau^\zeta(.)$ is the

Caputo derivative operator of non-integer order $\zeta, \zeta \in (0,1)$ and appropriate initial conditions are $\mathcal{N}(0) = \mathcal{N}_0 > 0, \mathcal{I}(0) = \mathcal{I}_0 > 0, \mathcal{P}(0) = \mathcal{P}_0 > 0$. A description of parameters in model (1.1) is seen in Table 1.1. Model (1.1) incorporates the effects of oncogenes and tumor suppressor genes through the growth rate of cancer cells λ, and the carrying capacity κ. It also includes the effects of immune cells through the parameter β_1 and the growth and spread of cancer cells through the parameters μ, γ, and δ. The role of blood vessels in delivering nutrients to cancer cells and promoting metastasis is captured through the parameter β_3. Finally, the effects of growth factors are captured through the parameters φ_1, φ_2, and φ_3. Lung cancer is a prevalent cancer worldwide and a leading cause of cancer-related mortality [44]. The disease is characterized by genetic mutations that result in uncontrolled cell growth and division, and its development is influenced by various factors such as smoking, environmental pollutants, and genetic predisposition [34]. However, the complexity of the disease has made the development of effective treatments challenging despite advancements in cancer research [28]. Amilo *et al.* [4] have discussed about local and global stability, reproduction number, and sensitivity of the suggested model.

In the current paper, first, classical Jacobi polynomials are transferred to the interval $[0, T]$. Then, the integral pseudo-operational matrix is constructed for the shifted Jacobi polynomials as basis functions. Using the operational matrix, appropriate approximations are derived for all terms in model (1.1). By substituting resultant approximations into equations in model (1.1), three residual functions are achieved that by collocating the residual functions at roots of the shifted Jacobi polynomial of degree $M + 1$, a non-linear system involving $3(M + 1)$ algebraic equations is obtained and by solving this system by Newton's iteration method, the unknown coefficients in series solutions are acquired approximately. With the investigation of the existence and uniqueness of solutions to model (1.1) by the Leray-Schauder fixed-point theorem, one can deal conveniently with the numerical solution of model (1.1) with the aid of the designed method. Some error bounds are estimated in a Jacobi-weighted L^2-space. By varying values of parameters in system (1.1), the sensitivity of the given model to parameters is studied. To gain better achievement and improve the results, a feedback control strategy is adopted by applying the method of Lagrange multipliers. For this purpose, after inputting appropriate control functions to model (1.1), an objective function is joined with three equations of the model as constraints. The target is to minimize the number of cancer cells and reduce their spread in lung tissues. Authors in [8, 9, 41] used generalized Bessel, Bernoulli, and Laguerre

Table 1.1: Description of parameters in model (1.1).

Parameter	**Description**
λ	Growth rate of lung cancer cells
κ	Carrying capacity of lung tissue
μ	Rate at which cancer cells spread from lung tissue to other parts of the body
β_1	Interaction between cancer cells and immune cells
$\varphi_1, \varphi_2, \varphi_3$	Effects of growth factors
β_2	Interaction between immune cells and growth of cancer cells
γ	Rate at which cancer cells in lung tissue spread to other parts of the body
δ	Rate of death of cancer cells that have spread to other parts of the body
β_3	Interaction between blood vessels and cancer cells

polynomials of the fractional orders to control and reduce the impact of cancer cells in the body. Indeed, they tried to control the behaviour of state variables by finding optimal values of fractional orders of basis functions. While in the current work, control variables are added to the given model in order to reduce the impact of the cancer cells.

The contributions of the current work are highlighted below:

- Classical Jacobi polynomials are extended to the interval $[0, T]$ and used to approximate solutions of model (1.1).
- A pseudo-operational collocation approach is designed to convert model (1.1) into a system of algebraic equations.
- The existence and uniqueness of solutions to the given model are proven using Leray-Schauder fixed-point theorem.
- Error bounds of spectral solutions obtained from the proposed method are estimated in a Jacobi-weighted space.
- Outputs are improved by adopting a feedback control strategy for the first time.

This paper is organized as follows. Section 2 is devoted to presenting definitions of fractional operators. Section 3 gives some theorems to prove the existence and uniqueness of solutions to model (1.1). In Section 4, a pseudo-operational integral matrix based on shifted Jacobi polynomials is derived. Estimating error bounds in a Jacobi-weighted space is presented in Section 5. The methodology involving finding spectral solutions to model (1.1), the sensitivity analysis, and giving a feedback control procedure is the subject of Section 6. Ultimately, the work ends with the discussion and conclusion in Sections 7 and 8.

2. Fractional Operators

Fractional calculus generalizes the integer-order calculus and fractional differentiation and integration operators have advantages in modeling diverse real-world phenomena. Here, some usable definitions and characteristics of fractional operators are recalled.

Definition 2.1. *The Riemann-Liouville fractional integral of non-integer order $\zeta > 0$ of a function $f(\tau) \in L^1([0, T])$ is defined as* [40]

$$ {}_0^{RL}\mathcal{I}_\tau^\zeta f(\tau) = \frac{1}{\Gamma(\zeta)} \int_0^\tau (\tau - \xi)^{\zeta - 1} f(\xi)\, d\xi, \quad \zeta > 0, \tag{2.1} $$

where Γ is the Gamma function. If $\zeta = 0$, then ${}_0^{RL}\mathcal{I}_\tau^\zeta f(\tau) = f(\tau)$.

Definition 2.2. *The fractional derivative operator in the Caputo concept of non-integer order $\zeta > 0$ of a function $f(\tau) \in C^n([0, T])$ is defined as* [40]

$$ {}_0^{C}\mathcal{D}_\tau^\zeta f(\tau) = \frac{1}{\Gamma(n - \zeta)} \int_0^\tau (\tau - \xi)^{n - \zeta - 1} f^{(n)}(\xi)\, d\xi, \quad n - 1 < \xi < n, \tag{2.2} $$

where

$$ f^{(n)}(\tau) = D^{(n)} f(\tau) = \frac{d^n f(\tau)}{d\tau^n}. $$

Some characteristics of fractional derivative and integral operators are listed as follows:

1. ${}_0^C\mathcal{D}_\tau^\zeta f(\tau) = {}_0^{RL}\mathcal{I}_\tau^{n-\zeta}\big(D^n f(\tau)\big), \quad D^n = \dfrac{d^n(.)}{d\tau^n}, \quad n-1 < \zeta < n,$
2. ${}_0^C\mathcal{D}_\tau^\zeta\big({}_0^{RL}\mathcal{I}_\tau^\zeta f(\tau)\big) = f(\tau),$
3. ${}_0^{RL}\mathcal{I}_\tau^\zeta\big({}_0^C\mathcal{D}_\tau^\zeta f(\tau)\big) = f(\tau) - \sum_{k=0}^{n-1} \dfrac{f^{(k)}(0)}{\Gamma(k+1)}\tau^k, \quad n-1 < \zeta < n,$
4. ${}_0^C\mathcal{D}^\zeta \tau^\alpha = \begin{cases} 0, & \lfloor\zeta\rfloor > \alpha, \\ \dfrac{\Gamma(\alpha+1)}{\Gamma(\alpha-\zeta+1)} t^{\alpha-\zeta}, & \text{otherwise}, \end{cases}$
5. ${}_0^{RL}\mathcal{I}^\zeta \tau^\alpha = \dfrac{\Gamma(\alpha+1)}{\Gamma(\alpha+\zeta+1)} t^{\alpha+\zeta}, \quad \alpha > 0,$

where $\zeta, \alpha \in \mathbb{R}$ and $n \in \mathbb{Z}^+$.

3. Existence and Uniqueness of Solutions

The Leray-Schauder fixed-point theorem [25] is used to prove the existence and uniqueness of the solution to system (1.1). First, assume $\mathcal{K}(\tau) = (\mathcal{N}(\tau), \mathcal{I}(\tau), \mathcal{P}(\tau))$, define the Banach space $\mathcal{A} = C(\mathbb{I}, \mathbb{R})^3, \mathbb{I} = [0, T]$, with the norm as

$$\|\mathcal{K}\|_{\mathcal{A}} = \|(\mathcal{N}, \mathcal{I}, \mathcal{P})\|_{\mathcal{A}} = \max_{\tau\in\mathbb{I}}\{|\mathcal{N}(\tau)| + |\mathcal{I}(\tau)| + |\mathcal{P}(\tau)|\}.$$

Rewrite the right-hand side of system (1.1) as follows:

$$\begin{cases} \mathcal{B}_1\big(\tau, \mathcal{N}(\tau), \mathcal{I}(\tau), \mathcal{P}(\tau)\big) = \lambda\mathcal{N}(\tau)\left(1 - \dfrac{\mathcal{N}(\tau)}{\kappa}\right) - \mu\mathcal{N}(\tau)\mathcal{P}(\tau) - \beta_1\mathcal{N}(\tau)\mathcal{I}(\tau), \\ \mathcal{B}_2\big(\tau, \mathcal{N}(\tau), \mathcal{I}(\tau), \mathcal{P}(\tau)\big) = \varphi_1\mathcal{I}_0 + \varphi_2\mathcal{N}^2(\tau) - \varphi_3\mathcal{I}(\tau) - \beta_2\mathcal{I}(\tau)\mathcal{P}(\tau), \\ \mathcal{B}_3\big(\tau, \mathcal{N}(\tau), \mathcal{I}(\tau), \mathcal{P}(\tau)\big) = \gamma\mathcal{N}(\tau)\,\mathcal{P}(\tau) - \delta\,\mathcal{P}(\tau) - \beta_3\mathcal{I}(\tau)\mathcal{P}(\tau), \end{cases} \tag{3.1}$$

So, system (1.1) is turned into the following equivalent system using (3.1):

$$\begin{cases} {}_0^C\mathcal{D}_\tau^\zeta\mathcal{N}(\tau) = \mathcal{B}_1\big(\tau, \mathcal{N}(\tau), \mathcal{I}(\tau), \mathcal{P}(\tau)\big), \\ {}_0^C\mathcal{D}_\tau^\zeta\mathcal{I}(\tau) = \mathcal{B}_2\big(\tau, \mathcal{N}(\tau), \mathcal{I}(\tau), \mathcal{P}(\tau)\big), \\ {}_0^C\mathcal{D}_\tau^\zeta\mathcal{P}(\tau) = \mathcal{B}_3\big(\tau, \mathcal{N}(\tau), \mathcal{I}(\tau), \mathcal{P}(\tau)\big), \end{cases} \tag{3.2}$$

and the compact form of system (3.2) is as

$$\begin{cases} {}_0^C\mathcal{D}_\tau^\zeta\mathcal{K}(\tau) = \mathbf{B}\big(\tau, \mathcal{K}(\tau)\big), \\ \mathcal{K}(0) = \mathcal{K}_0, \end{cases} \tag{3.3}$$

where $\mathcal{K}_0 = (\mathcal{N}_0, \mathcal{I}_0, \mathcal{P}_0)$ and

$$\mathbf{B}\big(\tau, \mathcal{K}(\tau)\big) = \begin{cases} \mathcal{B}_1\big(\tau, \mathcal{N}(\tau), \mathcal{I}(\tau), \mathcal{P}(\tau)\big), \\ \mathcal{B}_2\big(\tau, \mathcal{N}(\tau), \mathcal{I}(\tau), \mathcal{P}(\tau)\big), \\ \mathcal{B}_3\big(\tau, \mathcal{N}(\tau), \mathcal{I}(\tau), \mathcal{P}(\tau)\big). \end{cases} \tag{3.4}$$

By applying the Riemann-Liouville integral operator to (3.4), one gets

$$\mathcal{K}(\tau) = \mathcal{K}_0 + \frac{1}{\Gamma(\zeta)} \int_0^\tau (\tau - \xi)^{\zeta-1} \mathbf{B}\big(\xi, \mathcal{K}(\xi)\big)\, d\xi, \tag{3.5}$$

or equivalently

$$\begin{cases} \mathcal{N}(\tau) = \mathcal{N}_0 + \dfrac{1}{\Gamma(\zeta)} \displaystyle\int_0^\tau (\tau - \xi)^{\zeta-1} \mathcal{B}_1\big(\xi, \mathcal{N}(\xi), \mathcal{I}(\xi), \mathcal{P}(\xi)\big)\, d\xi, \\ \mathcal{I}(\tau) = \mathcal{I}_0 + \dfrac{1}{\Gamma(\zeta)} \displaystyle\int_0^\tau (\tau - \xi)^{\zeta-1} \mathcal{B}_2\big(\xi, \mathcal{N}(\xi), \mathcal{I}(\xi), \mathcal{P}(\xi)\big)\, d\xi, \\ \mathcal{P}(\tau) = \mathcal{P}_0 + \dfrac{1}{\Gamma(\zeta)} \displaystyle\int_0^\tau (\tau - \xi)^{\zeta-1} \mathcal{B}_3\big(\xi, \mathcal{N}(\xi), \mathcal{I}(\xi), \mathcal{P}(\xi)\big)\, d\xi. \end{cases} \tag{3.6}$$

Now, define the right-hand side of (3.5) as a mapping $\mathcal{F} : \mathcal{A} \to \mathcal{A}$ as follows:

$$\mathcal{F}\big(\mathcal{K}(\tau)\big) = \mathcal{K}_0 + \frac{1}{\Gamma(\zeta)} \int_0^\tau (\tau - \xi)^{\zeta-1} \mathbf{B}\big(\xi, \mathcal{K}(\xi)\big)\, d\xi. \tag{3.7}$$

To prove the existence of solutions to system (1.1), the Leray-Schauder fixed point theorem is used [25].

Theorem 3.1 (Leray-Schauder Fixed Point Theorem). *Let $\mathcal{A}$ be a Banach space, $\mathcal{E} \subset \mathcal{A}$ be a closed convex and bounded set, and $\mathcal{Q} \subset \mathcal{E}$ be an open set involving $0 \in \mathcal{Q}$. Then, under the compact and continuous mapping $\mathcal{F} : \bar{\mathcal{Q}} \to \mathcal{E}$, either*

$$\begin{aligned} &\text{C1}: \quad \exists\, z \in \bar{\mathcal{Q}} \quad s.t. \quad z = \mathcal{F}(z), \\ &\textit{or} \\ &\text{C2}: \quad \exists\, z \in \partial\mathcal{Q}, \quad \eta \in (0,1) \quad s.t. \quad z = \eta\, \mathcal{F}(z). \end{aligned}$$

Theorem 3.2 (Existence). *Suppose $\mathbf{B} \in C(\mathbb{I} \times \mathcal{A}, \mathcal{A})$. If*

$$\begin{aligned} &\text{P1}: \quad \exists\, \psi \in L^1(\mathbb{I}, \mathbb{R}^+) \text{ and } \exists\, \mathcal{L} \in C([0,\infty), [0,\infty)) \ (\mathcal{L} \text{ is non-decreasing}) \text{ such that} \\ &\qquad \forall\, \tau \in \mathbb{I} \text{ and } \mathcal{K} \in \mathcal{A}, \text{ one has } \big|\mathbf{B}(\tau, \mathcal{K}(\tau))\big| \le \psi(\tau)\mathcal{L}(|\mathcal{K}(\tau)|), \\ &\text{P2}: \quad \exists\, \varpi > 0 \text{ such that } \ \frac{\varpi}{\mathcal{K}_0 + T^\zeta/(\Gamma(\zeta+1))\psi_0^*\mathcal{L}(\varpi)} > 1 \quad \text{with } \psi_0^* = \sup_{\tau\in\mathbb{I}} |\psi(\tau)|, \end{aligned} \tag{3.8}$$

then there exists a set of solutions to the fractional lung cancer system (1.1).

Proof. Consider the mapping $\mathcal{F}$ defined in (3.7) and suppose $S_r = \{\mathcal{K} \in \mathcal{A} : \|\mathcal{K}\|_{\mathcal{A}} \le r\}$. Since $\mathbf{B}$ is continuous, therefore, $\mathcal{F}$ is continuous, as well. One gets from P1

$$\begin{aligned} \big|\mathcal{F}\big(\mathcal{K}(\tau)\big)\big| &\le \mathcal{K}_0 + \frac{1}{\Gamma(\zeta)} \int_0^\tau (\tau - \xi)^{\zeta-1} \big|\mathbf{B}\big(\xi, \mathcal{K}(\xi)\big)\big|\, d\xi \\ &\le \mathcal{K}_0 + \frac{1}{\Gamma(\zeta)} \int_0^\tau (\tau - \xi)^{\zeta-1} |\psi(\xi)|\, \mathcal{L}\big(|\mathcal{K}(\xi)|\big)\, d\xi \\ &\le \mathcal{K}_0 + \frac{T^\zeta}{\Gamma(\zeta+1)} \psi_0^* \mathcal{L}(r). \end{aligned}$$

So,

$$\|\mathcal{F}(\mathcal{K})\|_{\mathcal{A}} \le \mathcal{K}_0 + \frac{T^\zeta}{\Gamma(\zeta+1)} \psi_0^* \mathcal{L}(r) < \infty. \tag{3.9}$$

Thus, $\mathcal{F}$ is uniformly bounded on $\mathcal{A}$. Now, assume that $u, v \in [0, T]$ such that $u < v, \mathcal{K} \in S_r$, and

$$\mathbf{B}^* = \sup_{(\tau,\mathcal{K})\in\mathbb{I}\times S_r} \big|\mathbf{B}\big(\tau, \mathcal{K}(\tau)\big)\big| < \infty.$$

One has

$$\begin{aligned}
&\big|\mathcal{F}\big(\mathcal{K}(v)\big) - \mathcal{F}\big(\mathcal{K}(u)\big)\big| \\
&\leq \frac{1}{\Gamma(\zeta)}\bigg|\int_0^v (v-\xi)^{\zeta-1}\mathbf{B}\big(\xi, \mathcal{K}(\xi)\big)\, d\xi - \int_0^u (u-\xi)^{\zeta-1}\mathbf{B}\big(\xi, \mathcal{K}(\xi)\big)\, d\xi\bigg| \\
&\leq \frac{\mathbf{B}^*}{\Gamma(\zeta+1)}[v^{\zeta-1} - u^{\zeta-1}].
\end{aligned} \tag{3.10}$$

It can be seen that the right-hand side in (3.10) tends to zero as $v \to u$. Consequently, $\|\mathcal{F}(\mathcal{K}(v)) - \mathcal{F}(\mathcal{K}(u))\|_{\mathcal{A}} \to 0$ such that $v \to u$. Based on the Arzela-Ascoli theorem and compactness of $\mathcal{F}$ over $S_r, \mathcal{F}$ is equicontinuous. If the Leray-Schauder theorem is fulfilled on $\mathcal{F}$, one of C1 or C2 is satisfied. From C2, one can set $\Psi = \{\mathcal{K} \in \mathcal{A} \,|\, \|\mathcal{K}\|_{\mathcal{A}} = \varpi\}$ for some $\varpi > 0$ such that

$$\mathcal{K}_0 + \frac{T^\zeta}{\Gamma(\zeta+1)}\psi_0^*\mathcal{L}(\varpi) < \varpi.$$

From C1 and (3.9), one has

$$\|\mathcal{F}(\mathcal{K})\|_{\mathcal{A}} \leq \mathcal{K}_0 + \frac{T^\zeta}{\Gamma(\zeta+1)}\psi_0^*\mathcal{L}(\|\mathcal{K}\|_{\mathcal{A}}). \tag{3.11}$$

Assume that there are $\mathcal{K} \in \partial\Psi$ and $\eta \in (0, 1)$ such that $\mathcal{K} = \eta\,\mathcal{F}(\mathcal{K})$. Then, from (3.11) one can write

$$\begin{aligned}
\varpi = \|\mathcal{K}\|_{\mathcal{A}} &= \eta\,\|\mathcal{F}(\mathcal{K})\|_{\mathcal{A}} \\
&< \mathcal{K}_0 + \frac{T^\zeta}{\Gamma(\zeta+1)}\psi_0^*\mathcal{L}(\|\mathcal{K}\|_{\mathcal{A}}) \\
&< \mathcal{K}_0 + \frac{T^\zeta}{\Gamma(\zeta+1)}\psi_0^*\mathcal{L}(\varpi) < \varpi,
\end{aligned}$$

that is a contradiction. Therefore, C2 is not satisfied and $\mathcal{F}$ possesses a fixed point in $\bar{\Psi}$ based on the Leray-Schauder theorem. Thus, the existence of a solution to fractional lung cancer model (1.1) is proven. □

Now, we show that equations in system (1.1) have the Lipschitz property.

Lemma 3.1. *Assume that* $(\mathcal{N}, \mathcal{I}, \mathcal{P}), (\mathcal{N}^*, \mathcal{I}^*, \mathcal{P}^*) \in \mathcal{U} = C(\mathbb{I}, \mathbb{R})$ *and*

$$\begin{aligned}
\text{E1}: \quad &\|\mathcal{N}\| \leq \sigma_1, \quad \|\mathcal{I}\| \leq \sigma_2, \quad \|\mathcal{P}\| \leq \sigma_3, \quad \|\mathcal{N}^*\| \leq \sigma_1^*, \quad \|\mathcal{I}^*\| \leq \sigma_2^*, \quad \|\mathcal{P}^*\| \leq \sigma_3^*, \\
&\sigma_j, \sigma_j^* > 0, \quad j = 1, 2, 3.
\end{aligned}$$

Then, $\mathcal{B}_1, \mathcal{B}_2$, *and* $\mathcal{B}_3$ *in* (3.1) *satisfy the Lipschitz property with constants* $\gamma_1, \gamma_2, \gamma_3 > 0$ *with respect to appropriate arguments, where*

$$\gamma_1 = \lambda + \frac{\lambda}{\kappa} + 2\sigma_1^*\frac{\lambda}{\kappa} + \beta_1\sigma_2, \quad \gamma_2 = \varphi_3 + \beta_2\sigma_3, \quad \gamma_3 = \gamma\sigma_1 + \delta + \beta_3\sigma_2. \tag{3.12}$$

Proof. Consider $\mathcal{N},\mathcal{N}^* \in \mathcal{U} = C(\mathbb{I},\mathbb{R})$, so one has

$$\begin{aligned}
&\|\mathcal{B}_1(\tau,\mathcal{N},\mathcal{I},\mathcal{P}) - \mathcal{B}_1(\tau,\mathcal{N}^*,\mathcal{I},\mathcal{P})\| \\
&= \left\|\lambda(\mathcal{N}-\mathcal{N}^*) - \frac{\lambda}{\kappa}(\mathcal{N}^2-\mathcal{N}^{*2}) - \mu(\mathcal{N}\mathcal{P}-\mathcal{N}^*\mathcal{P}) - \beta_1(\mathcal{N}\mathcal{I}-\mathcal{N}^*\mathcal{I})\right\| \\
&\leq \lambda\|\mathcal{N}-\mathcal{N}^*\| + \frac{\lambda}{\kappa}\|\mathcal{N}-\mathcal{N}^*\|(\|\mathcal{N}-\mathcal{N}^*\| + 2\|\mathcal{N}^*\|) + \beta_1\|\mathcal{N}-\mathcal{N}^*\|\|\mathcal{I}\| \\
&\leq \lambda\|\mathcal{N}-\mathcal{N}^*\| + \frac{\lambda}{\kappa}\|\mathcal{N}-\mathcal{N}^*\|(\|\mathcal{N}-\mathcal{N}^*\| + 2\sigma_1^*) + \beta_1\sigma_2\|\mathcal{N}-\mathcal{N}^*\| \\
&= \left(\lambda + \frac{\lambda}{\kappa} + 2\sigma_1^*\frac{\lambda}{\kappa} + \beta_1\sigma_2\right)\|\mathcal{N}-\mathcal{N}^*\| \\
&= \gamma_1\|\mathcal{N}-\mathcal{N}^*\|,
\end{aligned}$$

where $\gamma_1 = \lambda + \lambda/\kappa + 2\sigma_1^*\lambda/\kappa + \beta_1\sigma_2$. Thus, $\mathcal{B}_1$ is Lipschitz with respect to $\mathcal{N}$. Choose $\mathcal{I},\mathcal{I}^* \in \mathcal{U}$ for $\mathcal{B}_2$,

$$\begin{aligned}
&\|\mathcal{B}_2(\tau,\mathcal{N},\mathcal{I},\mathcal{P}) - \mathcal{B}_2(\tau,\mathcal{N},\mathcal{I}^*,\mathcal{P})\| \\
&= \| - \varphi_3(\mathcal{I}-\mathcal{I}^*) - \beta_2(\mathcal{I}\mathcal{P}-\mathcal{I}^*\mathcal{P})\| \\
&\leq \varphi_3\|\mathcal{I}-\mathcal{I}^*\| + \beta_2\sigma_3\|\mathcal{I}-\mathcal{I}^*\| \\
&\leq (\varphi_3 + \beta_2\sigma_3)\|\mathcal{I}-\mathcal{I}^*\| \\
&= \gamma_2\|\mathcal{I}-\mathcal{I}^*\|,
\end{aligned}$$

where $\gamma_2 = \varphi_3 + \beta_2\sigma_3$. Similarly, for $\mathcal{B}_3$ one has

$$\begin{aligned}
&\|\mathcal{B}_3(\tau,\mathcal{N},\mathcal{I},\mathcal{P}) - \mathcal{B}_3(\tau,\mathcal{N},\mathcal{I},\mathcal{P}^*)\| \\
&= \|\gamma(\mathcal{N}\mathcal{P}-\mathcal{N}\mathcal{P}^*) - \delta(\mathcal{P}-\mathcal{P}^*) - \beta_3(\mathcal{I}\mathcal{P}-\mathcal{I}\mathcal{P}^*)\| \\
&\leq \gamma\sigma_1\|\mathcal{P}-\mathcal{P}^*\| + \delta\|\mathcal{P}-\mathcal{P}^*\| + \beta_3\sigma_2\|\mathcal{P}-\mathcal{P}^*\| \\
&= (\gamma\sigma_1 + \delta + \beta_3\sigma_2)\|\mathcal{P}-\mathcal{P}^*\| \\
&= \gamma_3\|\mathcal{P}-\mathcal{P}^*\|,
\end{aligned}$$

where $\gamma_3 = \gamma\sigma_1 + \delta + \beta_3\sigma_2$. Therefore, above inequalities show that $\mathcal{B}_1,\mathcal{B}_2$, and $\mathcal{B}_3$ are Lipschitz with respect to $\mathcal{N},\mathcal{I}$, and $\mathcal{P}$, respectively with $\gamma_j > 0, j = 1,2,3$. □

Theorem 3.3 (Uniqueness). *Suppose that* $\|\mathcal{N}\| \leq \sigma_1, \|\mathcal{I}\| \leq \sigma_2, \|\mathcal{P}\| \leq \sigma_3$ *and consider quantities in* (3.12). *If*

$$\frac{T^\zeta\,\gamma_j}{\Gamma(\zeta+1)} < 1, \quad j = 1,2,3, \tag{3.13}$$

then there exists exactly a set of solutions to fractional lung cancer model (1.1).

Proof. Suppose that there exist two solutions $(\mathcal{N},\mathcal{I},\mathcal{P})$ and $(\mathcal{N}^*,\mathcal{I}^*,\mathcal{P}^*)$ to system (1.1) under initial conditions $\mathcal{N}_0^* = \mathcal{N}_0, \mathcal{I}_0^* = \mathcal{I}_0$, and $\mathcal{P}_0^* = \mathcal{P}_0$. From (3.6), one has

$$\begin{cases}
\mathcal{N}^* = \mathcal{N}_0 + \dfrac{1}{\Gamma(\zeta)}\displaystyle\int_0^\tau (\tau-\xi)^{\zeta-1}\mathcal{B}_1\big(\xi,\mathcal{N}^*(\xi),\mathcal{I}^*(\xi),\mathcal{P}^*(\xi)\big)d\xi, \\
\mathcal{I}^* = \mathcal{I}_0 + \dfrac{1}{\Gamma(\zeta)}\displaystyle\int_0^\tau (\tau-\xi)^{\zeta-1}\mathcal{B}_2\big(\xi,\mathcal{N}^*(\xi),\mathcal{I}^*(\xi),\mathcal{P}^*(\xi)\big)d\xi, \\
\mathcal{P}^* = \mathcal{P}_0 + \dfrac{1}{\Gamma(\zeta)}\displaystyle\int_0^\tau (\tau-\xi)^{\zeta-1}\mathcal{B}_3\big(\xi,\mathcal{N}^*(\xi),\mathcal{I}^*(\xi),\mathcal{P}^*(\xi)\big)d\xi.
\end{cases}$$

So, one can estimate

$$\begin{aligned}\|\mathcal{N}-\mathcal{N}^*\| &\leq \frac{1}{\Gamma(\zeta)}\int_0^\tau (\tau-\xi)^{\zeta-1}\|\mathcal{B}_1(\xi,\mathcal{N},\mathcal{I},\mathcal{P})-\mathcal{B}_1(\xi,\mathcal{N}^*,\mathcal{I}^*,\mathcal{P}^*)\|d\xi\\ &\leq \frac{T^\zeta\,\gamma_1}{\Gamma(\zeta+1)}\|\mathcal{N}-\mathcal{N}^*\|.\end{aligned}$$

So,

$$\left(1-\frac{T^\zeta\,\gamma_1}{\Gamma(\zeta+1)}\right)\|\mathcal{N}-\mathcal{N}^*\|\leq 0.$$

From (3.13), one has $\mathcal{N}(\tau)-\mathcal{N}^*(\tau)$. One can obtain similarly,

$$\begin{aligned}\|\mathcal{I}-\mathcal{I}^*\| &\leq \frac{1}{\Gamma(\zeta)}\int_0^\tau (\tau-\xi)^{\zeta-1}\|\mathcal{B}_2(\xi,\mathcal{N},\mathcal{I},\mathcal{P})-\mathcal{B}_2(\xi,\mathcal{N}^*,\mathcal{I}^*,\mathcal{P}^*)\|d\xi\\ &\leq \frac{T^\zeta\,\gamma_2}{\Gamma(\zeta+1)}\|\mathcal{I}-\mathcal{I}^*\|,\\ \|\mathcal{P}-\mathcal{P}^*\| &\leq \frac{1}{\Gamma(\zeta)}\int_0^\tau (\tau-\xi)^{\zeta-1}\|\mathcal{B}_3(\xi,\mathcal{N},\mathcal{I},\mathcal{P})-\mathcal{B}_2(\xi,\mathcal{N}^*,\mathcal{I}^*,\mathcal{P}^*)\|d\xi\\ &\leq \frac{T^\zeta\,\gamma_3}{\Gamma(\zeta+1)}\|\mathcal{P}-\mathcal{P}^*\|.\end{aligned}$$

Using (3.13) leads to $\mathcal{I}^*=\mathcal{I},\mathcal{P}^*=\mathcal{P}$. Therefore, system (1.1) possesses a unique solution. □

4. Shifted Jacobi Polynomials over Interval [0, T] and Integral Pseudo-operational Matrix

Classical Jacobi polynomials, as a category of orthogonal polynomials, play a vital role in studying special functions and approximation theory [19]. These polynomials are denoted by $\mathsf{J}_i^{(\theta,\vartheta)}(t)$ and defined on the interval $[-1,1]$ where i refers to the degree of the given polynomial and θ,ϑ are two parameters greater than -1 which different choices of them yield different families of orthogonal polynomials, for instance, the Legendre polynomials ($\theta=\vartheta=0$), Chebyshev polynomials of the first kind ($\theta=\vartheta=-0.5$), Chebyshev polynomials of the second kind ($\theta=\vartheta=0.5$), and so on. Using the change of variable $\tau=2t/T-1$, the shifted version of Jacobi polynomials is achieved over the interval $[0,T]$, denoted by

$$\mathsf{J}_i^{(\theta,\vartheta)}\left(\frac{2t}{T}-1\right)=\mathsf{J}_i^{(\theta,\vartheta)}(\tau).$$

The shifted Jacobi polynomials satisfy the following three-term recurrence relation:

$$\begin{aligned}\mathsf{J}_i^{(\theta,\vartheta)}(\tau) &= \frac{(\theta+\vartheta+2i-1)\big(\theta^2-\vartheta^2+\tau(\theta+\vartheta+2i)(\theta+\vartheta+2i-2)\big)}{2i\,(\theta+\vartheta+i)(\theta+\vartheta+2i-2)}\mathsf{J}_{i-1}^{(\theta,\vartheta)}(\tau)\\ &\quad-\frac{(\theta+i-1)(\vartheta+i-1)(\theta+\vartheta+2i)}{i\,(\theta+\vartheta+i)(\theta+\vartheta+2i-2)}\mathsf{J}_{i-2}^{(\theta,\vartheta)}(\tau),\quad i=2,3,\ldots,\quad \tau\in[0,T],\end{aligned}\tag{4.1}$$

where the starting values are

$$\mathsf{J}_0^{(\theta,\vartheta)}(\tau)=1,\quad \mathsf{J}_1^{(\theta,\vartheta)}(\tau)=\frac{\theta+\vartheta+2}{2}\tau+\frac{\theta-\vartheta}{2},$$

and $\tau = 2t/T - 1$. One of the properties of the shifted Jacobi polynomials is orthogonality, i.e.

$$\int_0^T \mathsf{J}_j^{(\theta,\vartheta)}(\tau)\, \mathsf{J}_k^{(\theta,\vartheta)}(\tau)\, \omega^{(\theta,\vartheta)}(\tau)\, d\tau = \delta_{j,k}\, \bar{h}_j^{(\theta,\vartheta)},$$

where $\omega^{(\theta,\vartheta)}(\tau) = \tau^{\vartheta}(T-\tau)^{\theta}$ is the weight function, $\delta_{j,k}$ is the Kronecker delta function, and $\bar{h}_j^{(\theta,\vartheta)}$ is the normalization constant as follows:

$$\bar{h}_j^{(\theta,\vartheta)} = \frac{T^{\theta+\vartheta+1}\Gamma(\theta+j+1)\Gamma(\vartheta+j+1)}{(\theta+\vartheta+2j+1)\Gamma(j+1)\Gamma(\theta+\vartheta+j+1)}, \quad j = 0,1,2,\ldots. \tag{4.2}$$

In addition to relation (4.1), the shifted Jacobi polynomials are obtained from the following series:

$$\mathsf{J}_i^{(\theta,\vartheta)}(\tau) = \sum_{k=0}^{i} \gamma_k^{(i)}\, \tau^k, \quad i = 0,1,2,\ldots, \quad k = 0,1,\ldots,i, \tag{4.3}$$

where

$$\gamma_k^{(i)} = (-1)^{i-k} \frac{\Gamma(\vartheta+i+1)\Gamma(\theta+\vartheta+i+k+1)}{\Gamma(\vartheta+k+1)\Gamma(\theta+\vartheta+i+1)\Gamma(i-k+1)\Gamma(k+1)T^k},$$
$$i = 0,1,2,\ldots, \quad k = 0,1,\ldots,i.$$

Orthogonal polynomials constitute a basis in which continuous/squared integrable functions can be expanded using a linear combination of them. This allows an approximation of functions by truncating such series where the coefficients are obtained via inner products. To illustrate, consider the function $g(\tau) \in L^2_{\omega^{(\theta,\vartheta)}}(\mathbb{I}), \mathbb{I} = [0,T]$, where $L^2_{\omega^{(\theta,\vartheta)}}(\mathbb{I})$ is a Jacobi-weighted space. This function can be expanded in terms of the shifted Jacobi polynomials as follows:

$$g(\tau) = \sum_{k=0}^{\infty} \mathsf{g}_k\, \mathsf{J}_k^{(\theta,\vartheta)}(\tau), \tag{4.4}$$

where the coefficient g_k can be calculated using inner product

$$\mathsf{g}_k = \frac{1}{\bar{h}_k^{(\theta,\vartheta)}} \int_0^{\tau} g(\tau)\, \mathsf{J}_k^{(\theta,\vartheta)}(\tau)\, \omega^{(\theta,\vartheta)}(\tau)\, d\tau, \quad k = 0,1,2,\ldots.$$

To approximate solutions of a given functional equation, a truncated form of the series solution in (4.4) is used

$$g(\tau) \approx g_M(\tau) = \sum_{k=0}^{M} \mathsf{g}_k\, \mathsf{J}_k^{(\theta,\vartheta)}(\tau) = \mathsf{G}^{\top} \mathbb{J}^{(\theta,\vartheta)}(\tau), \tag{4.5}$$

where G and $\mathbb{J}^{(\theta,\vartheta)}(\tau)$ are the following $(M+1)\times 1$ vectors:

$$\mathsf{G} = [\mathsf{g}_0, \mathsf{g}_1, \mathsf{g}_2, \ldots, \mathsf{g}_M]^{\top}, \quad \mathbb{J}^{(\theta,\vartheta)}(\tau) = \left[\mathsf{J}_0^{(\theta,\vartheta)}(\tau), \mathsf{J}_1^{(\theta,\vartheta)}(\tau), \mathsf{J}_2^{(\theta,\vartheta)}(\tau), \ldots, \mathsf{J}_M^{(\theta,\vartheta)}(\tau)\right]^{\top}. \tag{4.6}$$

To avoid performing the integration operation to reduce computational costs, an operational procedure is constructed. Hence, an integral pseudo-operational matrix is derived based on shifted Jacobi polynomials. Consider the basis vector $\mathbb{J}^{(\theta,\vartheta)}(\tau)$ in (4.6). Applying the Riemann-Liouville integral operator to the mth component of the basis vector leads to

$${}_0^{RL}\mathcal{I}_{\tau}^{\zeta}\, \mathsf{J}_m^{(\theta,\vartheta)}(\tau) = \sum_{k=0}^{m} \gamma_k^{(m)} \frac{\Gamma(k+1)\tau^{k+\zeta}}{\Gamma(k+\zeta+1)} = \tau^{\zeta} \sum_{k=0}^{m} \gamma_k^{(m)} \frac{\Gamma(k+1)\tau^k}{\Gamma(k+\zeta+1)}, \quad m = 0,1,\ldots,M.$$

Now, τ^k is expanded in terms of basis functions

$$\tau^k \approx \sum_{i=0}^{M} d_i^{(k)}\, \mathsf{J}_i^{(\theta,\vartheta)}(\tau),$$

where the coefficient $d_i^{(k)}$ is calculated as follows:

$$\begin{aligned} d_i^{(k)} &= \frac{1}{\bar{h}_i^{(\theta,\vartheta)}} \int_0^T \tau^k\, \mathsf{J}_i^{(\theta,\vartheta)}(\tau)\, \omega^{(\theta,\vartheta)}(\tau)\, d\tau \\ &= \frac{1}{\bar{h}_i^{(\theta,\vartheta)}} \sum_{j=0}^{i} \gamma_j^{(i)} \int_0^T T^{\theta+\vartheta+k+j} \frac{\tau^{k+j+\theta}}{T^{k+j+\vartheta}} \left(1-\frac{\tau}{T}\right)^{\theta} d\tau \\ &= \frac{1}{\bar{h}_i^{(\theta,\vartheta)}} \sum_{j=0}^{i} \gamma_j^{(i)}\, T^{k+j+\theta+\vartheta+1} \int_0^1 u^{k+j+\vartheta}(1-u)^{\theta} du \\ &= \frac{1}{\bar{h}_i^{(\theta,\vartheta)}} \sum_{j=0}^{i} \gamma_j^{(i)}\, T^{k+j+\theta+\vartheta+1} \frac{\Gamma(k+j+\vartheta+1)\,\Gamma(\theta+1)}{\Gamma(k+j+\theta+\vartheta+2)}. \end{aligned}$$

So, one has

$$\begin{aligned} &{}_0^{RL}\mathcal{I}_\tau^{\zeta}\, \mathsf{J}_m^{(\theta,\vartheta)}(\tau) \\ &\approx \tau^{\zeta} \sum_{i=0}^{M} \left\{ \sum_{k=0}^{m} \sum_{j=0}^{i} \frac{T^{\theta+\vartheta+k+j+1} \gamma_k^{(m)}\, \gamma_j^{(i)}\, \Gamma(k+1)\,\Gamma(k+j+\vartheta+1)\,\Gamma(\theta+1)}{\bar{h}_i^{(\theta,\vartheta)}\,\Gamma(k+\zeta+1)\,\Gamma(k+j+\theta+\vartheta+2)} \right\} \mathsf{J}_i^{(\theta,\vartheta)}(\tau) \end{aligned}$$

for $m = 0, 1, \ldots, M, i = 0, 1, \ldots, m$. Therefore, the integration of the basis vector in a matrix form will be displayed as follows:

$${}_0^{RL}\mathcal{I}_\tau^{\zeta}\, \mathbb{J}^{(\theta,\vartheta)}(\tau) \approx \tau^{\zeta}\, \Lambda^{(\zeta,\theta,\vartheta)}\, \mathbb{J}^{(\theta,\vartheta)}(\tau), \tag{4.7}$$

where $\Lambda^{(\zeta,\theta,\vartheta)}$ is the following integral pseudo-operational matrix:

$$\Lambda^{(\zeta,\theta,\vartheta)} = \begin{bmatrix} \lambda_{0,0}^{(\zeta,\theta,\vartheta)} & \lambda_{0,1}^{(\zeta,\theta,\vartheta)} & \cdots & \lambda_{0,M}^{(\zeta,\theta,\vartheta)} \\ \lambda_{1,0}^{(\zeta,\theta,\vartheta)} & \lambda_{1,1}^{(\zeta,\theta,\vartheta)} & \cdots & \lambda_{1,M}^{(\zeta,\theta,\vartheta)} \\ \vdots & \vdots & \ddots & \vdots \\ \lambda_{M,0}^{(\zeta,\theta,\vartheta)} & \lambda_{M,1}^{(\zeta,\theta,\vartheta)} & \cdots & \lambda_{M,M}^{(\zeta,\theta,\vartheta)} \end{bmatrix},$$

and its entries are calculated as

$$\lambda_{m,i}^{(\zeta,\theta,\vartheta)} = \sum_{k=0}^{m} \sum_{j=0}^{i} \frac{T^{\theta+\vartheta+k+j+1} \gamma_k^{(m)}\, \gamma_j^{(i)}\, \Gamma(k+1)\,\Gamma(k+j+\vartheta+1)\,\Gamma(\theta+1)}{\bar{h}_i^{(\theta,\vartheta)}\,\Gamma(k+\zeta+1)\,\Gamma(k+j+\theta+\vartheta+2)}, \quad m, i = 0, 1, \ldots, M.$$

Appropriate approximations are substituted in the given equations to obtain residual functions. These residual functions are collocated at roots of the shifted Jacobi polynomial of degree $M+1$ and a non-linear system of algebraic equations, including $3(M+1)$ algebraic equations, is achieved. By solving the resultant algebraic system, the vectors of coefficients in the series solutions are derived approximately, so, approximate spectral solutions of model (1.1) are acquired.

5. Error Bounds

Suppose that $\mathsf{Z}(\tau)$ is a sufficiently smooth function over the interval $[0,T]$ and $\mathsf{Q}_M(\tau)$ is an interpolating polynomial to $\mathsf{Z}(\tau)$, therefore one has

$$\mathsf{Z}(\tau)-\mathsf{Q}_M(\tau)=\frac{\mathsf{Z}^{(M+1)}(\xi)}{\Gamma(M+2)}\prod_{n=0}^{M}(\tau-\tau_n),\quad \xi\in(0,T),$$

where $\tau_n, n=0,1,\ldots,M$ are roots of the shifted Chebyshev polynomials of the first kind of degree $M+1$ over $[0,T]$. If $\max_{\tau\in[0,T]}|\mathsf{Z}^{(M+1)}(\tau)|=\mathcal{M}_{\mathsf{Z}}$, then one has [37]

$$\|\mathsf{Z}-\mathsf{Q}_M\|_{L^2_{\omega^{(\theta,\vartheta)}}(\mathbb{I})}\leq\frac{\mathcal{M}_{\mathsf{Z}}\,T^{M+1}}{2^{2M+1}\,\Gamma(M+2)},\tag{5.1}$$

where $\|.\|_{L^2_{\omega^{(\theta,\vartheta)}}(\mathbb{I})}$ is the L^2-norm in the Jacobi-weighted space $\mathcal{A}_{\omega^{(\theta,\vartheta)}}$, which are defined as follows:

$$\mathcal{A}_{\omega^{(\theta,\vartheta)}}=\left\{\mathsf{f}(\tau)\in L^2_{\omega^{(\theta,\vartheta)}}(\mathbb{I})\;\middle|\;\left\|\frac{d^k\mathsf{f}(\tau)}{d\tau^k}\right\|_{L^2_{\omega^{(\theta+k,\vartheta+k)}}(\mathbb{I})}<\infty\right\},$$
$$\|\mathsf{f}\|_{L^2_{\omega^{(\theta,\vartheta)}}(\mathbb{I})}=\left(\int_0^T\mathsf{f}^2(\tau)\,\omega^{(\theta,\vartheta)}(\tau)\,d\tau\right)^{\frac{1}{2}}.$$

Theorem 5.1. *Suppose that $\mathsf{Z}(\tau)\in\mathcal{A}_{\omega^{(\theta,\vartheta)}}$ is an $(M+1)$-time continuously differentiable function on the interval $[0,T]$, $\mathsf{Z}_M(\tau)=\mathsf{C}^\top\mathbb{J}^{(\theta,\vartheta)}(\tau)$ is the expansion of $\mathsf{Z}(\tau)$ in terms of shifted Jacobi polynomials, and $\widetilde{\mathsf{Z}}_M(\tau)=\widetilde{\mathsf{C}}^\top\mathbb{J}^{(\theta,\vartheta)}(\tau)$ is the approximate solution obtained from the suggested scheme. Then, one gets*

$$\|\mathsf{Z}-\widetilde{\mathsf{Z}}_M\|_{L^2_{\omega^{(\theta,\vartheta)}}(\mathbb{I})}\leq\frac{\mathcal{M}_{\mathsf{Z}}\,T^{M+\frac{\theta+\vartheta+3}{2}}}{2^{2M+1}\,\Gamma(M+2)}\sqrt{\frac{\Gamma(\theta+1)\Gamma(\vartheta+1)}{\Gamma(\theta+\vartheta+2)}}+\|\mathsf{C}-\widetilde{\mathsf{C}}\|_2\left(\sum_{n=0}^{M}\bar{h}_n^{(\theta,\vartheta)}\right)^{\frac{1}{2}}.\tag{5.2}$$

Proof. Let $\mathbb{G}_M$ be the space of all polynomials of degree at most M. So, $\mathsf{Z}_M(\tau),\widetilde{\mathsf{Z}}_M(\tau)\in\mathbb{G}_M$. One can write

$$\|\mathsf{Z}-\widetilde{\mathsf{Z}}_M\|_{L^2_{\omega^{(\theta,\vartheta)}}(\mathbb{I})}\leq\|\mathsf{Z}-\mathsf{Z}_M\|_{L^2_{\omega^{(\theta,\vartheta)}}(\mathbb{I})}+\|\mathsf{Z}_M-\widetilde{\mathsf{Z}}_M\|_{L^2_{\omega^{(\theta,\vartheta)}}(\mathbb{I})}.\tag{5.3}$$

Now, some upper bounds are calculated for the norms on the right side in (5.3). From (5.1), one gets

$$\begin{aligned}&\|\mathsf{Z}-\mathsf{Z}_M\|_{L^2_{\omega^{(\theta,\vartheta)}}(\mathbb{I})}\\&\leq\|\mathsf{Z}-\mathsf{Q}_M\|_{L^2_{\omega^{(\theta,\vartheta)}}(\mathbb{I})}=\left(\int_0^T|\mathsf{Z}(\tau)-\mathsf{Q}_M(\tau)|^2\omega^{(\theta,\vartheta)}(\tau)d\tau\right)^{\frac{1}{2}}\\&\leq\left(\int_0^T\left(\frac{\mathcal{M}_{\mathsf{Z}}\,T^{M+1}}{2^{2M+1}\Gamma(M+2)}\right)^2\omega^{(\theta,\vartheta)}(\tau)d\tau\right)^{\frac{1}{2}}\\&=\frac{\mathcal{M}_{\mathsf{Z}}T^{M+(\theta+\vartheta+3)/2}}{2^{2M+1}\Gamma(M+2)}\sqrt{\frac{\Gamma(\theta+1)\Gamma(\vartheta+1)}{\Gamma(\theta+\vartheta+2)}}.\end{aligned}\tag{5.4}$$

Using Cauchy-Schwarz's inequality, one has

$$\begin{aligned}
&\|\mathsf{Z}_M - \widetilde{\mathsf{Z}}_M\|^2_{L^2_{\omega^{(\theta,\vartheta)}}(\mathbb{I})} \\
&= \int_0^T \left[\sum_{n=0}^{M}(\mathsf{C}_n - \widetilde{\mathsf{C}}_n)\mathsf{J}_n^{(\theta,\vartheta)}(\tau)\right]^2 \omega^{(\theta,\vartheta)}(\tau)d\tau \\
&\leq \left(\sum_{n=0}^{M}(\mathsf{C}_n - \widetilde{\mathsf{C}}_n)^2\right)^{\frac{1}{2}}\left(\int_0^T\left(\sum_{n=0}^{M}\mathsf{J}_n^{(\theta,\vartheta)^2}(\tau)\omega^{(\theta,\vartheta)}(\tau)\right)d\tau\right)^{\frac{1}{2}} \\
&= \|\mathsf{C} - \widetilde{\mathsf{C}}\|_2\sqrt{\sum_{n=0}^{M}\bar{h}_n^{(\theta,\vartheta)}},
\end{aligned}$$

where $\|\cdot\|_2$ is the Euclidean norm of the given scalar vector $\mathsf{W} = [w_1, w_2, \ldots, w_m]^\top$, i.e.

$$\|\mathsf{W}\|_2 = \left(\sum_{k=0}^{m}|w_k|^2\right)^{\frac{1}{2}}.$$

Therefore, one can get upper bound (5.2) for the inequality in (5.3). □

Assume that $\mathcal{N}_M(\tau), \mathcal{I}_M(\tau)$, and $\mathcal{P}_M(\tau)$ are approximate solutions to model (1.1) obtained from the pseudo-operational collocation method. By applying the Riemann-Liouville integral operator to system (1.1), one gets the following system:

$$\begin{cases}
\mathcal{N}(\tau) = \mathcal{N}_0 + \dfrac{1}{\Gamma(\zeta)}\displaystyle\int_0^\tau (\tau-\zeta)^{\zeta-1}\left[\lambda\mathcal{N}(\xi) - \frac{\lambda}{\kappa}\mathcal{N}^2(\xi) - \mu\mathcal{N}(\xi)\mathcal{P}(\xi) - \beta_1\mathcal{N}(\xi)\mathcal{I}(\xi)\right]d\xi, \\
\mathcal{I}(\tau) = \mathcal{I}_0 + \dfrac{1}{\Gamma(\zeta)}\displaystyle\int_0^\tau (\tau-\zeta)^{\zeta-1}\left[\phi_1\mathcal{I}_0 + \phi_2\mathcal{N}^2(\xi) - \phi_3\mathcal{I}(\xi) - \beta_2\mathcal{I}(\xi)\mathcal{P}(\xi)\right]d\xi, \\
\mathcal{P}(\tau) = \mathcal{P}_0 + \dfrac{1}{\Gamma(\zeta)}\displaystyle\int_0^\tau (\tau-\zeta)^{\zeta-1}\left[\gamma\mathcal{N}(\xi)\mathcal{P}(\xi) - \delta\mathcal{P}(\xi) - \beta_3\mathcal{I}(\xi)\mathcal{P}(\xi)\right]d\xi.
\end{cases} \tag{5.5}$$

If $\mathcal{N}_M(\tau), \mathcal{I}_M(\tau)$, and $\mathcal{P}_M(\tau)$ are approximate solutions to system (1.1) obtained from the suggested method, then one has the following approximate system:

$$\begin{cases}
\mathcal{N}_M(\tau) = \mathcal{N}_0 + \mathcal{H}_\mathcal{N}(\tau) + \dfrac{1}{\Gamma(\zeta)}\displaystyle\int_0^\tau (\tau-\zeta)^{\zeta-1}\Big[\lambda\mathcal{N}_M(\xi) - \frac{\lambda}{\kappa}\mathcal{N}_M^2(\xi) - \mu\mathcal{N}_M(\xi)\mathcal{P}_M(\xi) \\
\qquad\qquad - \beta_1\mathcal{N}_M(\xi)\mathcal{I}_M(\xi)\Big]d\xi, \\
\mathcal{I}_M(\tau) = \mathcal{I}_0 + \mathcal{H}_\mathcal{I}(\tau) + \dfrac{1}{\Gamma(\zeta)}\displaystyle\int_0^\tau (\tau-\zeta)^{\zeta-1}\left[\phi_1\mathcal{I}_0 + \phi_2\mathcal{N}_M^2(\xi) - \phi_3\mathcal{I}_M(\xi)\right. \\
\qquad\qquad \left. - \beta_2\mathcal{I}_M(\xi)\mathcal{P}_M(\xi)\right]d\xi, \\
\mathcal{P}_M(\tau) = \mathcal{P}_0 + \mathcal{H}_\mathcal{P}(\tau) + \dfrac{1}{\Gamma(\zeta)}\displaystyle\int_0^\tau (\tau-\zeta)^{\zeta-1}\left[\gamma\mathcal{N}_M(\xi)\mathcal{P}_M(\xi) - \delta\mathcal{P}_M(\xi)\right. \\
\qquad\qquad \left. - \beta_3\mathcal{I}_M(\xi)\mathcal{P}_M(\xi)\right]d\xi,
\end{cases} \tag{5.6}$$

where $\mathcal{H}_\mathcal{N}(\tau), \mathcal{H}_\mathcal{I}(\tau)$, and $\mathcal{H}_\mathcal{P}(\tau)$ are residual functions. Subtracting Eq. (5.6) from Eq. (5.5) and defining error functions as

$$e_\mathcal{N}(\tau) = \mathcal{N}(\tau) - \mathcal{N}_M(\tau), \quad e_\mathcal{I}(\tau) = \mathcal{I}(\tau) - \mathcal{I}_M(\tau), \quad e_\mathcal{P}(\tau) = \mathcal{P}(\tau) - \mathcal{P}_M(\tau)$$

lead to the following error equations:

$$\begin{cases} \mathcal{H}_{\mathcal{N}}(\tau) = e_{\mathcal{N}}(\tau) - \dfrac{1}{\Gamma(\zeta)} \\ \qquad \times \displaystyle\int_0^\tau (\tau-\zeta)^{\zeta-1}\Big[\lambda\, e_{\mathcal{N}}(\xi) - \frac{\lambda}{\kappa} e_{\mathcal{N}}(\xi)\big(e_{\mathcal{N}}(\xi) + 2\mathcal{N}_M(\xi)\big) \\ \qquad\qquad -\mu\big(e_{\mathcal{N}}(\xi)\big(e_{\mathcal{P}}(\xi) + \mathcal{P}_M(\xi)\big) + \mathcal{N}_M(\xi) e_{\mathcal{P}}(\xi)\big) \\ \qquad\qquad -\beta_1\big(e_{\mathcal{N}}(\xi)\big(e_{\mathcal{I}}(\xi) + \mathcal{I}_M(\xi)\big) + \mathcal{N}_M(\xi) e_{\mathcal{I}}(\xi)\big)\Big] d\xi, \\ \mathcal{H}_{\mathcal{I}}(\tau) = e_{\mathcal{I}}(\tau) - \dfrac{1}{\Gamma(\zeta)} \\ \qquad \times \displaystyle\int_0^\tau (\tau-\zeta)^{\zeta-1}\big[\varphi_2\, e_{\mathcal{N}}(\xi)\big(e_{\mathcal{N}}(\xi) + 2\mathcal{N}_M(\xi)\big) - \varphi_3\, e_{\mathcal{I}}(\xi) \\ \qquad\qquad -\beta_2\big(e_{\mathcal{I}(\xi)}\big(e_{\mathcal{P}}(\xi) + \mathcal{P}_M(\xi)\big) + \mathcal{I}_M(\xi) e_{\mathcal{P}}(\xi)\big)\big] d\xi, \\ \mathcal{H}_{\mathcal{P}}(\tau) = e_{\mathcal{P}}(\tau) - \dfrac{1}{\Gamma(\zeta)} \\ \qquad \times \displaystyle\int_0^\tau (\tau-\zeta)^{\zeta-1}\big[\gamma\big(e_{\mathcal{N}}(\xi)\big(e_{\mathcal{P}}(\xi) + \mathcal{P}_M(\xi)\big) + \mathcal{N}_M(\xi) e_{\mathcal{P}}(\xi)\big) \\ \qquad\qquad -\delta e_{\mathcal{P}}(\xi) - \beta_3\big(e_{\mathcal{I}}(\xi)\big(e_{\mathcal{P}}(\xi) + \mathcal{P}_M(\xi)\big) + \mathcal{I}_M(\xi) e_{\mathcal{P}}(\xi)\big)\big] d\xi. \end{cases} \tag{5.7}$$

Using resultant bounds in (5.2) leads to the following inequalities for the residual functions in (5.7):

$$\begin{aligned} \|\mathcal{H}_{\mathcal{N}}\|_{L^2_{\omega(\theta,\vartheta)}(\mathbb{I})} &\le \|e_{\mathcal{N}}\|_{L^2_{\omega(\theta,\vartheta)}(\mathbb{I})} + \frac{T^\zeta}{\Gamma(\zeta+1)} \\ &\quad \times \Big[\lambda\|e_{\mathcal{N}}\|_{L^2_{\omega(\theta,\vartheta)}(\mathbb{I})} + \frac{\lambda}{\kappa}\|e_{\mathcal{N}}\|_{L^2_{\omega(\theta,\vartheta)}(\mathbb{I})}\Big(\|e_{\mathcal{N}}\|_{L^2_{\omega(\theta,\vartheta)}(\mathbb{I})} + 2\|\mathcal{N}_M\|_\infty\Big) \\ &\qquad + \mu\Big(\|e_{\mathcal{N}}\|_{L^2_{\omega(\theta,\vartheta)}(\mathbb{I})}\Big(\|e_{\mathcal{P}}\|_{L^2_{\omega(\theta,\vartheta)}(\mathbb{I})} + \|\mathcal{P}_M\|_\infty\Big) + \|\mathcal{P}_M\|_\infty\|e_{\mathcal{P}}\|_{L^2_{\omega(\theta,\vartheta)}(\mathbb{I})}\Big) \\ &\qquad + \beta_1\Big(\Big(\|e_{\mathcal{I}}\|_{L^2_{\omega(\theta,\vartheta)}(\mathbb{I})} + \|\mathcal{I}_M\|_\infty\Big)\|e_{\mathcal{N}}\|_{L^2_{\omega(\theta,\vartheta)}(\mathbb{I})} + \|\mathcal{N}_M\|_\infty\|e_{\mathcal{I}}\|_{L^2_{\omega(\theta,\vartheta)}(\mathbb{I})}\Big)\Big], \\ \|\mathcal{H}_{\mathcal{I}}\|_{L^2_{\omega(\theta,\vartheta)}(\mathbb{I})} &\le \|e_{\mathcal{I}}\|_{L^2_{\omega(\theta,\vartheta)}(\mathbb{I})} + \frac{T^\zeta}{\Gamma(\zeta+1)} \\ &\quad \times \Big[\varphi_2\|e_{\mathcal{N}}\|_{L^2_{\omega(\theta,\vartheta)}(\mathbb{I})}\Big(\|e_{\mathcal{N}}\|_{L^2_{\omega(\theta,\vartheta)}(\mathbb{I})} + 2\|\mathcal{N}_M\|_\infty\Big) + \varphi_3\|e_{\mathcal{I}}\|_{L^2_{\omega(\theta,\vartheta)}(\mathbb{I})} \\ &\qquad + \beta_3\Big(\Big(\|e_{\mathcal{P}}\|_{L^2_{\omega(\theta,\vartheta)}(\mathbb{I})} + \|\mathcal{P}_M\|_\infty\Big)\|e_{\mathcal{I}}\|_{L^2_{\omega(\theta,\vartheta)}(\mathbb{I})} + \|\mathcal{I}_M\|_\infty\|e_{\mathcal{P}}\|_{L^2_{\omega(\theta,\vartheta)}(\mathbb{I})}\Big)\Big], \\ \|\mathcal{H}_{\mathcal{P}}\|_{L^2_{\omega(\theta,\vartheta)}(\mathbb{I})} &\le \|e_{\mathcal{P}}\|_{L^2_{\omega(\theta,\vartheta)}(\mathbb{I})} + \frac{T^\zeta}{\Gamma(\zeta+1)} \\ &\quad \times \Big[\gamma\Big(\|e_{\mathcal{P}}\|_{L^2_{\omega(\theta,\vartheta)}(\mathbb{I})} + \|\mathcal{P}_M\|_\infty\Big)\|e_{\mathcal{N}}\|_{L^2_{\omega(\theta,\vartheta)}(\mathbb{I})} + \|\mathcal{N}_M\|_\infty\|e_{\mathcal{P}}\|_{L^2_{\omega(\theta,\vartheta)}(\mathbb{I})} \\ &\qquad + \delta\|e_{\mathcal{P}}\|_{L^2_{\omega(\theta,\vartheta)}(\mathbb{I})} + \beta_3\Big(\Big(\|e_{\mathcal{P}}\|_{L^2_{\omega(\theta,\vartheta)}(\mathbb{I})} + \|\mathcal{P}_M\|_\infty\Big)\|e_{\mathcal{I}}\|_{L^2_{\omega(\theta,\vartheta)}(\mathbb{I})} \\ &\qquad\qquad + \|\mathcal{I}_M\|_\infty\|e_{\mathcal{P}}\|_{L^2_{\omega(\theta,\vartheta)}(\mathbb{I})}\Big)\Big]. \end{aligned}$$

It can be seen from the right-hand sides of the above inequalities, when the number of basis functions increases, the error bounds will be small enough. Then, we expect approximate solutions to be reliable.

6. Solution Method and Approximate Results

In this section, the suggested technique and control strategies are performed on model (1.1). All experiments are carried out utilizing Maple 2023 on a laptop with 3.00 GHz central processing unit, Intel (R) Core (TM) i5-7520U CPU, 8 GB memory, and Windows 11 operating system.

6.1. Solving model (1.1) by the suggested method

First, the terms involving fractional derivatives in model (1.1) are approximated as follows:

$$ {}_0^C\mathcal{D}_0^{\zeta}\mathcal{N}(\tau) \approx \mathsf{C}_1^{\top}\mathbb{J}^{(\theta,\vartheta)}(\tau), \quad {}_0^C\mathcal{D}_0^{\zeta}\mathcal{I}(\tau) \approx \mathsf{C}_2^{\top}\mathbb{J}^{(\theta,\vartheta)}(\tau), \quad {}_0^C\mathcal{D}_0^{\zeta}\mathcal{P}(\tau) \approx \mathsf{C}_3^{\top}\mathbb{J}^{(\theta,\vartheta)}(\tau), \tag{6.1} $$

where $\mathsf{C}_j, j = 1, 2, 3$ are unknown coefficients vectors which can be determined and $\mathbb{J}^{(\theta,\vartheta)}(\tau)$ is the basis vector in (4.6). Employing the Riemann-Liouville integral operator on approximations (6.1) and using the pseudo-operational matrix (4.7) result in the following approximations to $\mathcal{N}(\tau), \mathcal{I}(\tau)$, and $\mathcal{P}(\tau)$:

$$ \begin{aligned} \mathcal{N}(\tau) &\approx \mathcal{N}_0 + \tau^{\zeta}\mathsf{C}_1^{\top}\Lambda^{(\zeta,\theta,\vartheta)}\,\mathbb{J}^{(\theta,\vartheta)}(\tau), \\ \mathcal{I}(\tau) &\approx \mathcal{I}_0 + \tau^{\zeta}\mathsf{C}_2^{\top}\Lambda^{(\zeta,\theta,\vartheta)}\,\mathbb{J}^{(\theta,\vartheta)}(\tau), \\ \mathcal{P}(\tau) &\approx \mathcal{P}_0 + \tau^{\zeta}\mathsf{C}_3^{\top}\Lambda^{(\zeta,\theta,\vartheta)}\,\mathbb{J}^{(\theta,\vartheta)}(\tau). \end{aligned} \tag{6.2} $$

Now, substituting approximations (6.2) into system (1.1) yields the following residual functions:

$$ \begin{aligned} \mathcal{R}_1(\tau) &= \mathsf{C}_1^{\top}\mathbb{J}^{(\theta,\vartheta)}(\tau) - \lambda\big(\mathcal{N}_0+\tau^{\zeta}\mathsf{C}_1^{\top}\Lambda^{(\zeta,\theta,\vartheta)}\mathbb{J}^{(\theta,\vartheta)}(\tau)\big)\left(1-\frac{1}{\kappa}\big(\mathcal{N}_0+\tau^{\zeta}\mathsf{C}_1^{\top}\Lambda^{(\zeta,\theta,\vartheta)}\mathbb{J}^{(\theta,\vartheta)}(\tau)\big)\right) \\ &\quad + \mu\big(\mathcal{N}_0 + \tau^{\zeta}\mathsf{C}_1^{\top}\Lambda^{(\zeta,\theta,\vartheta)}\mathbb{J}^{(\theta,\vartheta)}(\tau)\big)\big(\mathcal{P}_0 + \tau^{\zeta}\mathsf{C}_3^{\top}\Lambda^{(\zeta,\theta,\vartheta)}\mathbb{J}^{(\theta,\vartheta)}(\tau)\big) \\ &\quad + \beta_1\big(\mathcal{N}_\prime + \tau^{\zeta}\mathsf{C}_1^{\top}\Lambda^{(\zeta,\theta,\vartheta)}\mathbb{J}^{(\theta,\vartheta)}(\tau)\big)\big(\mathcal{I}_0 + \tau^{\zeta}\mathsf{C}_2^{\top}\Lambda^{(\zeta,\theta,\vartheta)}\mathbb{J}^{(\theta,\vartheta)}(\tau)\big), \\ \mathcal{R}_2(\tau) &= \mathsf{C}_2^{\top}\mathbb{J}^{(\theta,\vartheta)}(\tau) - \varphi_1\mathcal{I}_0 - \varphi_2\big(\mathcal{N}_0 + \tau^{\zeta}\mathsf{C}_1^{\top}\Lambda^{(\zeta,\theta,\vartheta)}\mathbb{J}^{(\theta,\vartheta)}(\tau)\big)^2 \\ &\quad + \varphi_3\big(\mathcal{I}_0 + \tau^{\zeta}\mathsf{C}_2^{\top}\Lambda^{(\zeta,\theta,\vartheta)}\mathbb{J}^{(\theta,\vartheta)}(\tau)\big) \\ &\quad + \beta_2\big(\mathcal{I}_0 + \tau^{\zeta}\mathsf{C}_2^{\top}\Lambda^{(\zeta,\theta,\vartheta)}\mathbb{J}^{(\theta,\vartheta)}(\tau)\big)\big(\mathcal{P}_0 + \tau^{\zeta}\mathsf{C}_3^{\top}\Lambda^{(\zeta,\theta,\vartheta)}\mathbb{J}^{(\theta,\vartheta)}(\tau)\big), \\ \mathcal{R}_3(\tau) &= \mathsf{C}_3^{\top}\mathbb{J}^{(\theta,\vartheta)}(\tau) - \gamma\big(\mathcal{N}_0 + \tau^{\zeta}\mathsf{C}_1^{\top}\Lambda^{(\zeta,\theta,\vartheta)}\mathbb{J}^{(\theta,\vartheta)}(\tau)\big)\big(\mathcal{P}_0 + \tau^{\zeta}\mathsf{C}_3^{\top}\Lambda^{(\zeta,\theta,\vartheta)}\mathbb{J}^{(\theta,\vartheta)}(\tau)\big) \\ &\quad + \delta\big(\mathcal{P})0 + \tau^{\zeta}\mathsf{C}_3^{\top}\Lambda^{(\zeta,\theta,\vartheta)}\mathbb{J}^{(\theta,\vartheta)}(\tau)\big) \\ &\quad + \beta_3\big(\mathcal{I}_0 + \tau^{\zeta}\mathsf{C}_2^{\top}\Lambda^{(\zeta,\theta,\vartheta)}\mathbb{J}^{(\theta,\vartheta)}(\tau)\big)\big(\mathcal{P}_0 + \tau^{\zeta}\mathsf{C}_3^{\top}\Lambda^{(\zeta,\theta,\vartheta)}\mathbb{J}^{(\theta,\vartheta)}(\tau)\big). \end{aligned} \tag{6.3} $$

Now, by collocating the residual functions in (6.3) at $M+1$ roots of $\mathsf{J}_{M+1}^{(\theta,\vartheta)}(\tau)$ after choosing values of parameters θ and ϑ, a non-linear system involving $3(M+1)$ non-linear algebraic equations are obtained, by solving the resultant system via Newton's iteration method, values of unknown coefficients $\mathsf{C}_1, \mathsf{C}_2$, and C_3 are calculated approximately, then approximate solutions are achieved from (6.2).

In order to draw figures of approximations obtained for state variables $\mathcal{N}(\tau), \mathcal{I}(\tau)$, and $\mathcal{P}(\tau)$, the following initial values and values of parameters are considered [4]:

$$ \begin{aligned} &\mathcal{N}_0 = 35, \quad \mathcal{I}_0 = 9, \quad \mathcal{P}_0 = 3, \quad T = 10, \quad \lambda = 0.3, \\ &\kappa = 10000, \quad \mu = 0.01, \quad \beta_1 = 0.01, \quad \beta_2 = 0.01, \quad \beta_3 = 0.04, \\ &\varphi_1 = 0.03, \quad \varphi_2 = 0.04, \quad \varphi_3 = 0.01, \quad \gamma = 0.07, \quad \delta = 0.001. \end{aligned} \tag{6.4} $$

Figures of state variables in system (1.1) are depicted in Figs. 6.1-6.4 for $M = 7$, different values of θ and ϑ and $\zeta((\theta, \vartheta) = (0, 0), (0.5, 0.5), (1, 1), (-0.4, -0.25)$, $\zeta = 0.1, 0.2, 0.3, 0.4, 0.5)$. The target of modeling the growth of cancer cells in lung tissues is to adopt a strategy for controlling and reducing the propagation of cancer cells. As seen in Figs. 6.1-6.4, the number of cancer cells is reduced by the increase of the order of fractional derivative ζ. The number of immune cells

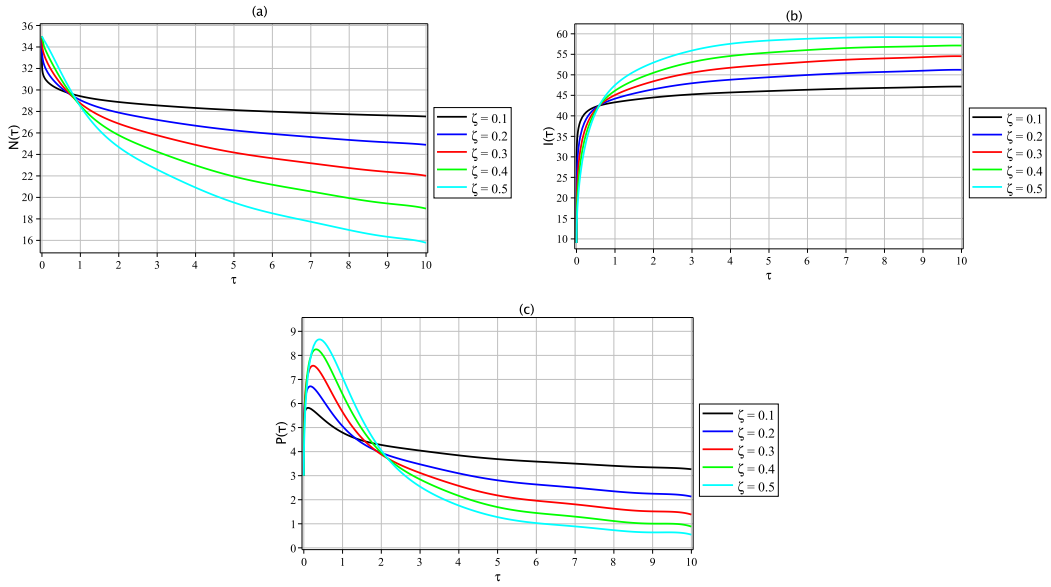

Fig. 6.1. Plots of approximate solutions to model (1.1): (a) $\mathcal{N}(\tau)$, (b) $\mathcal{I}(\tau)$, (c) $\mathcal{P}(\tau)$ for $(\theta, \vartheta) = (0, 0)$ and $M = 7$.

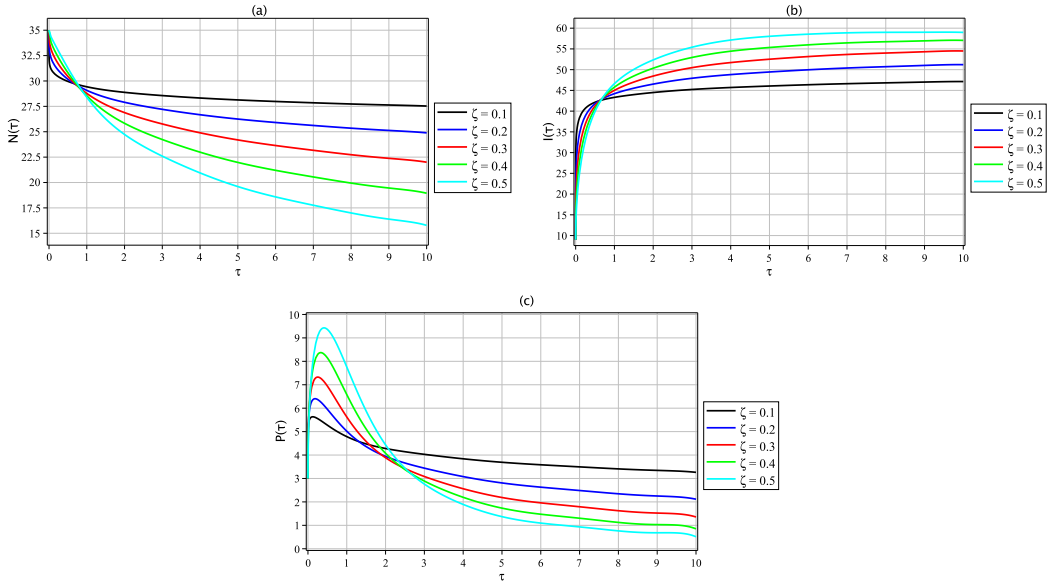

Fig. 6.2. Plots of approximate solutions to model (1.1): (a) $\mathcal{N}(\tau)$, (b) $\mathcal{I}(\tau)$, (c) $\mathcal{P}(\tau)$ for $(\theta, \vartheta) = (0.5, 0.5)$ and $M = 7$.

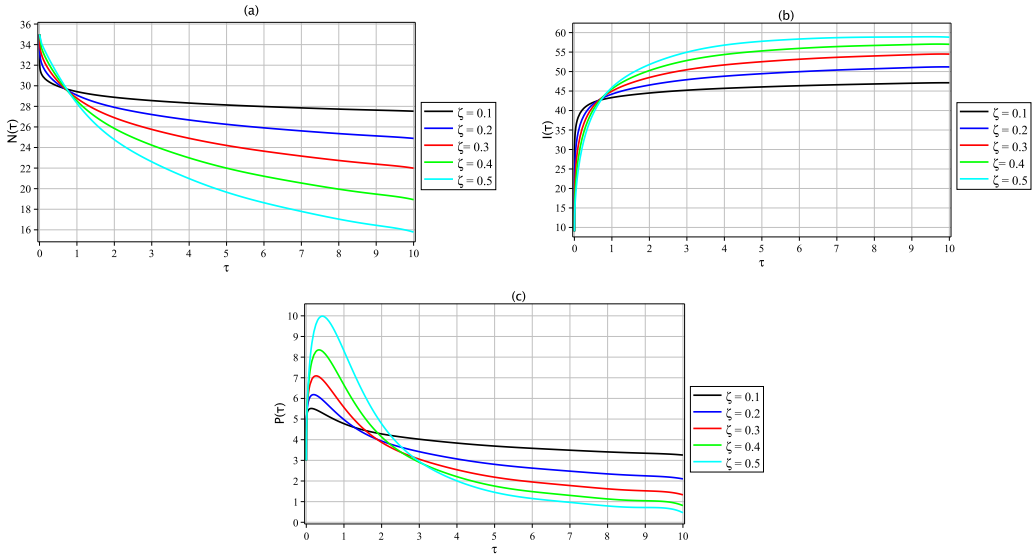

Fig. 6.3. Plots of approximate solutions to model (1.1): (a) $\mathcal{N}(\tau)$, (b) $\mathcal{I}(\tau)$, (c) $\mathcal{P}(\tau)$ for $(\theta, \vartheta) = (1, 1)$ and $M = 7$.

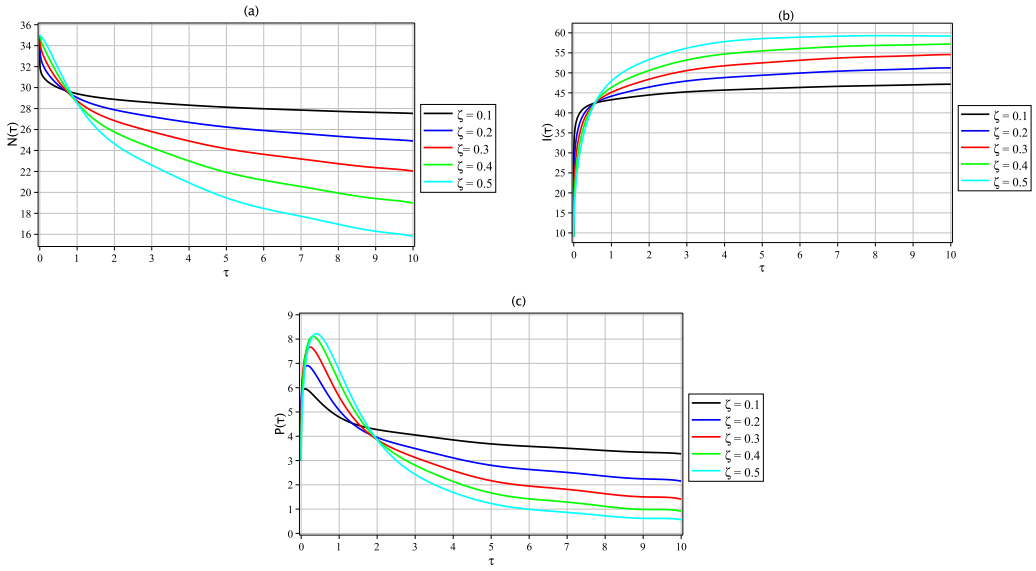

Fig. 6.4. Plots of approximate solutions to model (1.1): (a) $\mathcal{N}(\tau)$, (b) $\mathcal{I}(\tau)$, (c) $\mathcal{P}(\tau)$ for $(\theta, \vartheta) = (-0.4, -0.25)$ and $M = 7$.

is increasing and tending to $\mathcal{I}(\tau) = 60$ by increasing values of ζ. Values of $\mathcal{I}(\tau)$ sound constant after $\tau = 6$ for different values of ζ. The number of cancer cells spread to other parts of the body is first increasing up to for instance $\mathcal{P}(\tau) = 8.7$ for $(\theta, \vartheta) = (0, 0)$, while the maximum value of $\mathcal{P}(\tau)$ is $9.5, 10$, and 8.1 for $(\theta, \vartheta) = (0.5, 0.5), (1, 1), (-0.4, -0.5)$, respectively. And after $\tau = 0.5$, values of $\mathcal{P}(\tau)$ decrease and tend to 0.5. State variables $\mathcal{N}(\tau)$ and $\mathcal{I}(\tau)$ have similar behaviors by choosing different values of θ and ϑ for Jacobi polynomials.

6.2. Sensitivity analysis

The sensitivity analysis plays a pivotal role in appraising the soundness and reliability of mathematical models across various disciplines. It helps in distinguishing which parameters have the most operative effect on outputs of the given model. By figuring out the sensitivity of the given model to different parameters, researchers can optimize the model structure or parameter values to achieve better performance.

In this subsection, some scenarios will be designed to demonstrate the sensitivity of the suggested model to diverse parameters:

1. Sensitivity to λ. By choosing values of λ as $\lambda = 0.1, 0.2, 0.3, 0.4$, model (1.1) is solved by the method stated in the previous subsection and figures of $\mathcal{N}(\tau), \mathcal{I}(\tau)$, and $\mathcal{P}(\tau)$ are depicted in Fig. 6.5 for $M = 7, (\theta, \vartheta) = (1, 1)$, and $\zeta = 0.6$. From Fig. 6.5(a), the number of cancer cells decreases by increasing values of λ, but by setting values less than $\lambda = 0.3$, better results are achieved. The number of immune cells are increasing with the increase of values of λ till $\tau = 0.5$ and after that has a decreasing behaviour. The rate of propagation of cancer in lung tissues increases by raising values of λ, while after $\tau = 2.5$, all curves obey the same treatment.

2. Sensitivity to μ. By Choosing values $\mu = 0.01, 0.015, 0.02, 0.025$, solutions of the given system are approximated using the proposed scheme and figures of approximate solutions are seen in Fig. 6.6. The number of cancer cells is decreasing by increasing values of μ. All curves in Fig. 6.6(b) are increasing but by increasing values of μ, the number of immune cells decreases. The number of cancer cells spread in other parts of the body decreases after $\tau = 0.5$ and curves get close to the horizontal axis.

3. Sensitivity to β_1. Figures of $\mathcal{N}(\tau), \mathcal{I}(\tau)$, and $\mathcal{P}(\tau)$ are plotted and seen for β_1=0.01, 0.015, 0.02, 0.025 in Fig. 6.7. Values of $\mathcal{N}(\tau)$ decrease by increasing values of β_1, but the number of immune cells decreases considerably as well. The number of spread cancer cells for $\beta_1 = 0.025$ is less than other values over $[0, 3]$, but after $\tau = 3$ values of $\mathcal{P}(\tau)$ increase gradually.

4. Sensitivity to φ_1. By changing values of φ_1 ($\varphi_1 = 0.01, 0.02, 0.03, 0.04$), there is no change in the outputs as can be seen in Fig. 6.8.

5. Sensitivity to φ_2. By selecting values of φ_2 as $\varphi_2 = 0.02, 0.03, 0.04, 0.05$, undesirable results are gained for $\varphi_2 = 0.02$ and the number of cancer cells decreases for $\varphi_2 = 0.03, 0.04, 0.05$. While the number of immune cells increases by increasing values of φ_2. In Fig. 6.9(c), a decreasing treatment can be observed for $\varphi_2 = 0.03, 0.04, 0.05$.

6. Sensitivity to φ_3. From Fig. 6.10, by choosing different values for φ_3 ($\varphi_3 = 0.01, 0.02, 0.03$, 0.04), there is no significant change in the behaviour of state variables.

7. Sensitivity to β_2. From Fig. 6.11, increasing values of β_2 ($\varphi_3 = 0.01, 0.02, 0.03, 0.04$) can not be a good strategy because the number of cancer cells and the rate of propagation of them to other parts of the body increase. As seen, the number of immune cells decreases naturally.

8. Sensitivity to γ. By raising values of γ ($\gamma = 0.05, 0.06, 0.07, 0.078$) cancer cells are propagated to the other parts of the body increases, and the number of immune cells decreases. So, the increase of the values of γ is not a good idea. The behavior of the state functions are seen in Fig. 6.12.

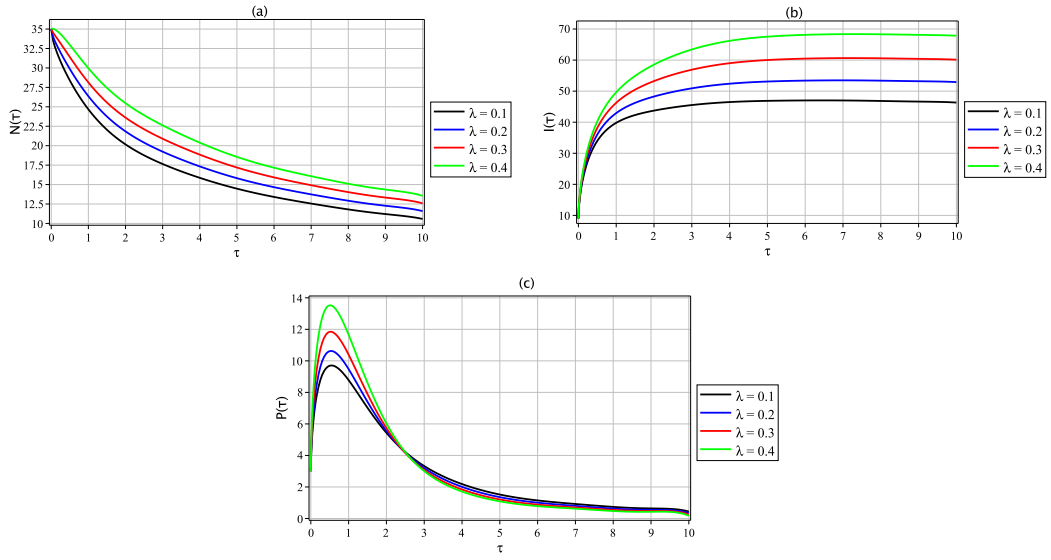

Fig. 6.5. Plots of approximate solutions to model (1.1): (a) $\mathcal{N}(\tau)$, (b) $\mathcal{I}(\tau)$, (c) $\mathcal{P}(\tau)$ for different values of λ, $\zeta = 0.6$, $(\theta, \vartheta) = (1, 1)$, and $M = 7$.

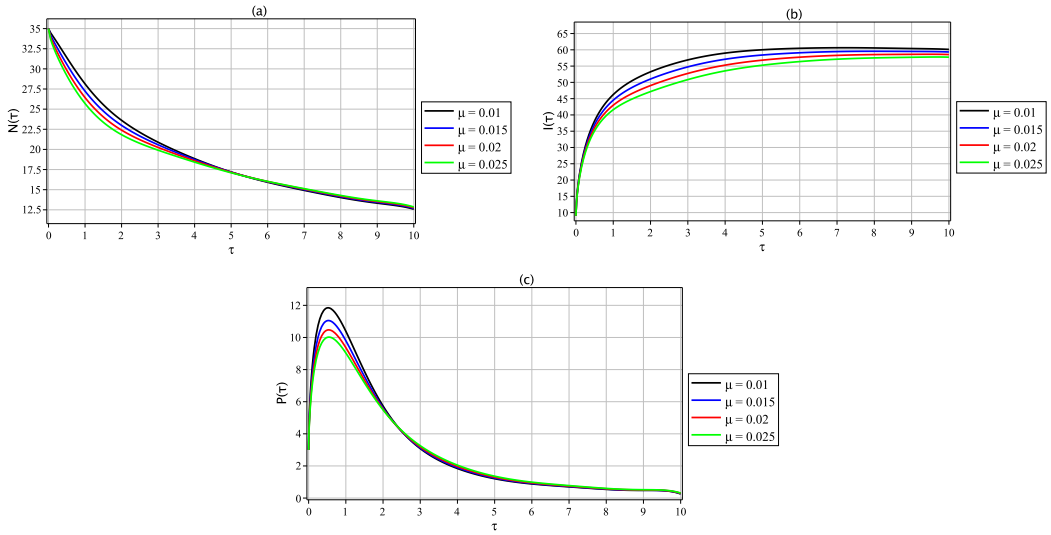

Fig. 6.6. Plots of approximate solutions to model (1.1): (a) $\mathcal{N}(\tau)$, (b) $\mathcal{I}(\tau)$, (c) $\mathcal{P}(\tau)$ for different values of μ, $\zeta = 0.6$, $(\theta, \vartheta) = (1, 1)$, and $M = 7$.

9. Sensitivity to δ. All curves in Figs. 6.13(a) and 6.13(b) coincide for $\delta = 0.001, 0.01, 0.05$, 0.1, while the number of cancer cells spread in the body decreases with the increase of values of δ.

10. Sensitivity to β_3. In Fig. 6.14, results are not desirable for $\beta_3 = 0.02$. The number of cancer cells, $\mathcal{N}(\tau)$, and the number of cancer cells spread in different parts of the body, $\mathcal{P}(\tau)$, decrease and the number of immune cells raises for $\beta_3 = 0.03, 0.04, 0.05$.

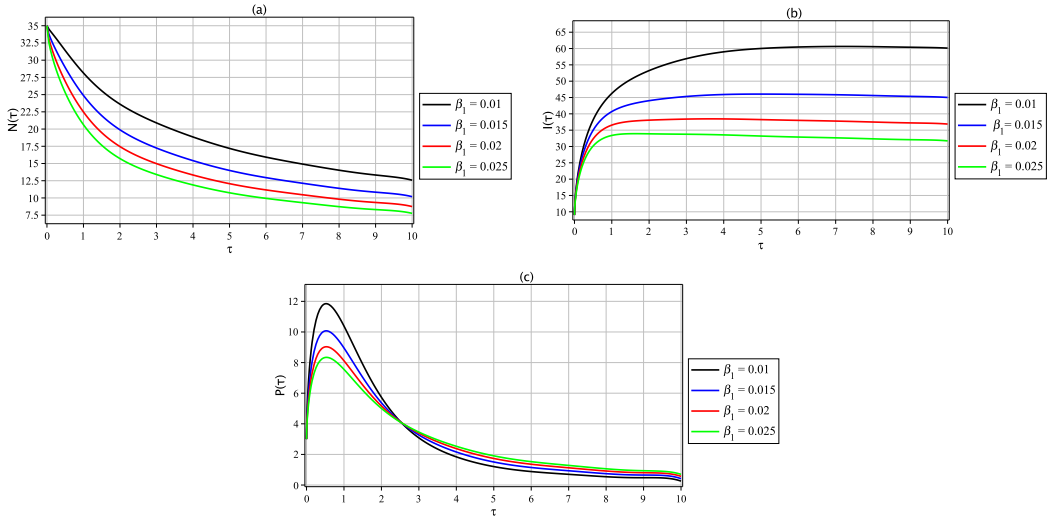

Fig. 6.7. Plots of approximate solutions to model (1.1): (a) $\mathcal{N}(\tau)$, (b) $\mathcal{I}(\tau)$, (c) $\mathcal{P}(\tau)$ for different values of β_1, $\zeta = 0.6$, $(\theta, \vartheta) = (1, 1)$, and $M = 7$.

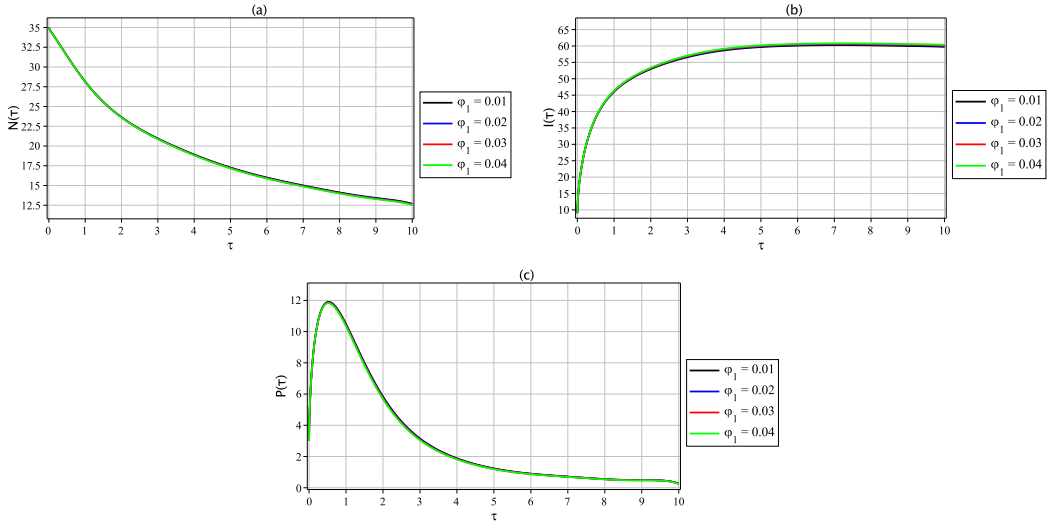

Fig. 6.8. Plots of approximate solutions to model (1.1): (a) $\mathcal{N}(\tau)$, (b) $\mathcal{I}(\tau)$, (c) $\mathcal{P}(\tau)$ for different values of φ_1, $\zeta = 0.6$, $(\theta, \vartheta) = (1, 1)$, and $M = 7$.

6.3. Feedback control strategy

Feedback control techniques help to improve the efficiency of the obtained outputs and the performance of the given system (1.1). In this subsection, a modified version of model (1.1) is considered with three control inputs $u_1(\tau), u_2(\tau)$, and $u_3(\tau)$ as time-dependent functions that should be minimized to diminish the spread of the cancer cells and to augment the immune

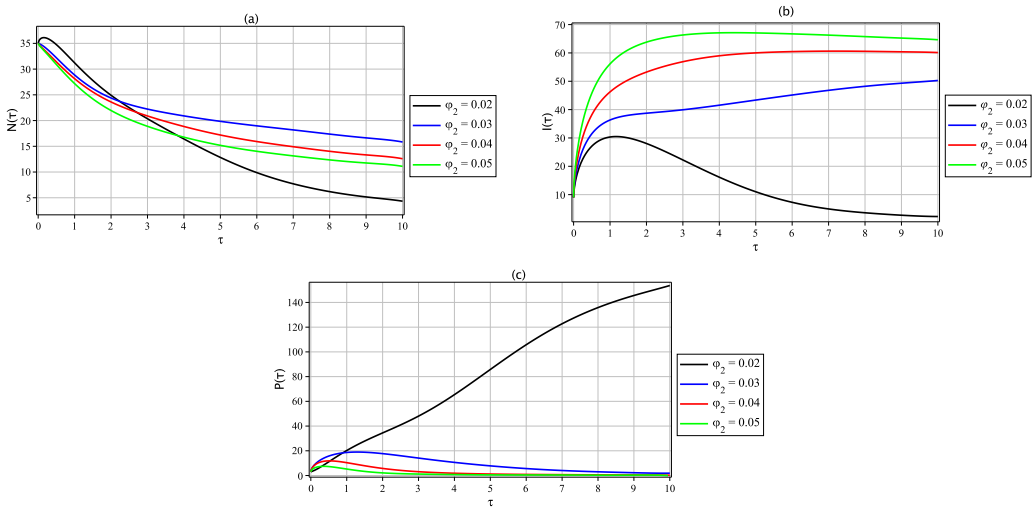

Fig. 6.9. Plots of approximate solutions to model (1.1): (a) $\mathcal{N}(\tau)$, (b) $\mathcal{I}(\tau)$, (c) $\mathcal{P}(\tau)$ for different values of φ_2, $\zeta = 0.6$, $(\theta, \vartheta) = (1, 1)$, and $M = 7$.

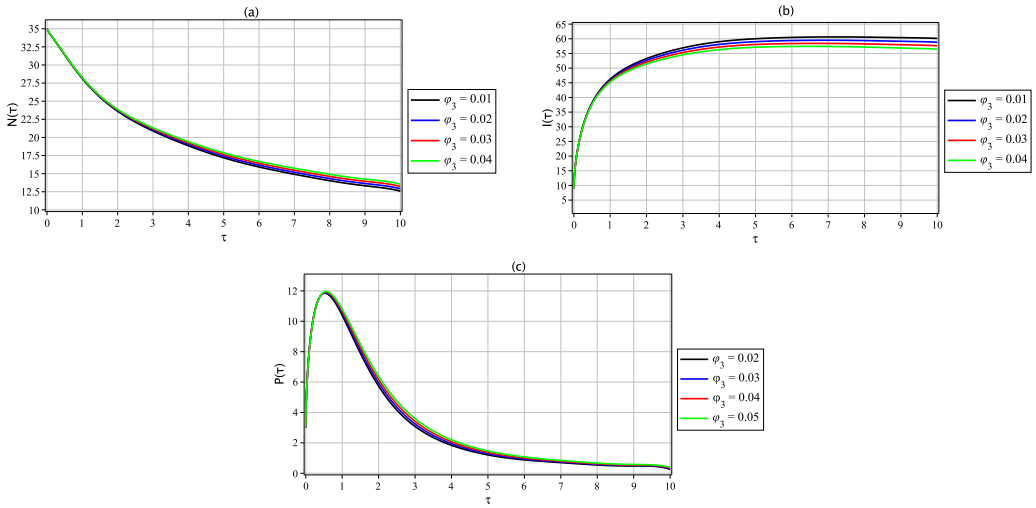

Fig. 6.10. Plots of approximate solutions to model (1.1): (a) $\mathcal{N}(\tau)$, (b) $\mathcal{I}(\tau)$, (c) $\mathcal{P}(\tau)$ for different values of φ_3, $\zeta = 0.6$, $(\theta, \vartheta) = (1, 1)$, and $M = 7$.

cells in lung tissues. The improved lung cancer model is seen below

$$\begin{cases} {}_0^C\mathcal{D}_\tau^\zeta \mathcal{N}(\tau) = \lambda\,\mathcal{N}(\tau)\left(1 - \dfrac{\mathcal{N}(\tau)}{\kappa}\right) - \mu\,\mathcal{N}(\tau)\mathcal{P}(\tau) - \beta_1\,\mathcal{N}(\tau)\mathcal{I}(\tau) - \xi_1\,u_1(\tau)\,\mathcal{N}(\tau), \\ {}_0^C\mathcal{D}_\tau^\zeta \mathcal{I}(\tau) = \varphi_1\,\mathcal{I}_0 + \varphi_2\,\mathcal{N}^2(\tau) - \varphi_3\,\mathcal{I}(\tau) - \beta_2\,\mathcal{I}(\tau)\mathcal{P}(\tau) + \xi_2\,u_2(\tau)\,\mathcal{I}(\tau), \\ {}_0^C\mathcal{D}_\tau^\zeta \mathcal{P}(\tau) = \gamma\,\mathcal{N}(\tau)\,\mathcal{P}(\tau) - \delta\,\mathcal{P}(\tau) - \beta_3\,\mathcal{I}(\tau)\mathcal{P}(\tau) - \xi_3\,u_3(\tau)\,\mathcal{P}(\tau), \end{cases} \tag{6.5}$$

and the corresponding objective function is given as follows:

$$\mathcal{F}(\mathcal{N}, \mathcal{I}, \mathcal{P}, u_1, u_2, u_3)$$

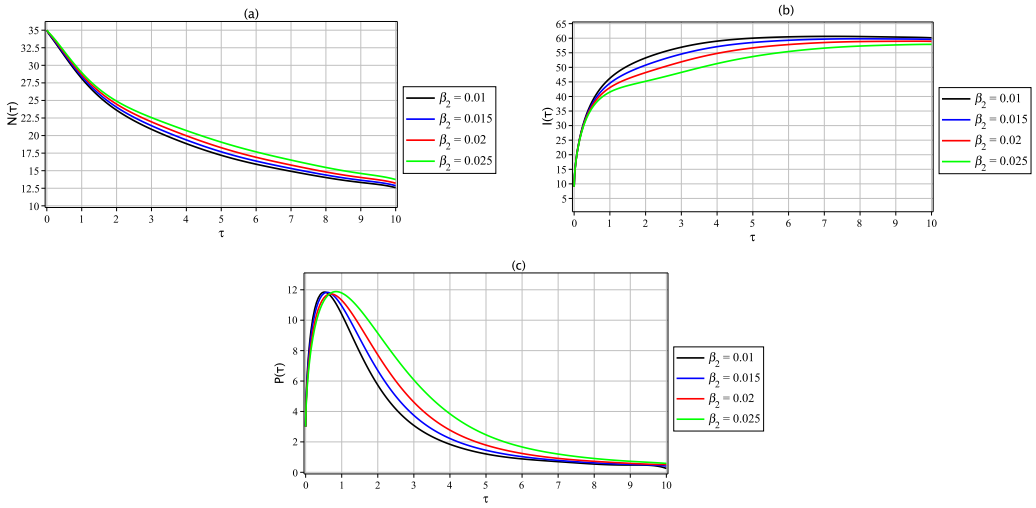

Fig. 6.11. Plots of approximate solutions to model (1.1): (a) $\mathcal{N}(\tau)$, (b) $\mathcal{I}(\tau)$, (c) $\mathcal{P}(\tau)$ for different values of β_2, $\zeta = 0.6$, $(\theta, \vartheta) = (1, 1)$, and $M = 7$.

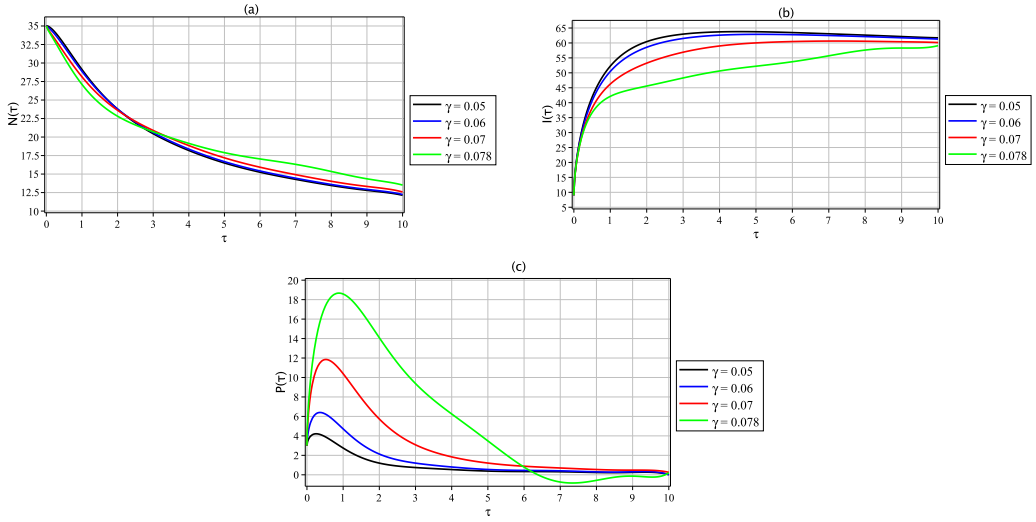

Fig. 6.12. Plots of approximate solutions to model (1.1): (a) $\mathcal{N}(\tau)$, (b) $\mathcal{I}(\tau)$, (c) $\mathcal{P}(\tau)$ for different values of γ, $\zeta = 0.6$, $(\theta, \vartheta) = (1, 1)$, and $M = 7$.

$$= \min \int_0^T \left(\eta_1 \mathcal{N}(\tau) - \eta_2 \mathcal{I}(\tau) + \eta_3 \mathcal{P}(\tau) + \epsilon_1 u_1^2(\tau) + \epsilon_2 u_2^2(\tau) + \epsilon_3 u_3^2(\tau) \right) d\tau, \tag{6.6}$$

where $\tau \in [0, T]$, $\eta_i, i = 1, 2, 3$ and $\epsilon_j, j = 1, 2, 3$ are weights to balance all terms in the integrand in (6.6) and must be determined to decrease the growth of cancer cells $(\mathcal{N}, \mathcal{P})$ and increase the number of immune cells $(\mathcal{I})$. The method of Lagrange multipliers is utilized to minimize the objective function (6.6) subject to constraints (6.5) [5]. To apply the proposed approach to model (6.5), the following approximations to control functions and approximations presented by (6.1) and (6.2) are required:

$$u_1(\tau) \approx U_1^\top \mathbb{J}^{(\theta,\vartheta)}(\tau), \quad u_2(\tau) \approx U_2^\top \mathbb{J}^{(\theta,\vartheta)}(\tau), \quad u_3(\tau) \approx U_3^\top \mathbb{J}^{(\theta,\vartheta)}(\tau), \tag{6.7}$$

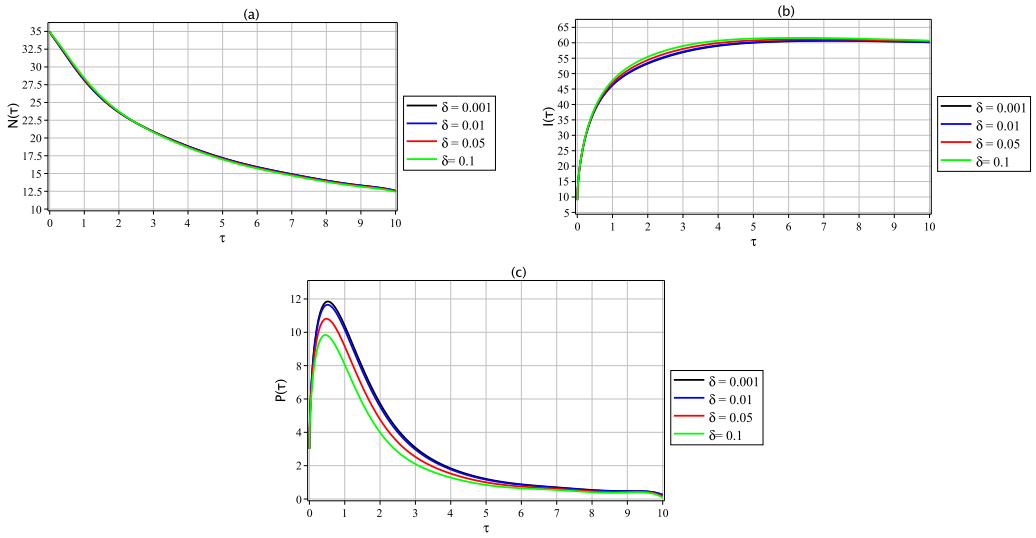

Fig. 6.13. Plots of approximate solutions to model (1.1): (a) $\mathcal{N}(\tau)$, (b) $\mathcal{I}(\tau)$, (c) $\mathcal{P}(\tau)$ for different values of δ, $\zeta = 0.6$, $(\theta, \vartheta) = (1, 1)$, and $M = 7$.

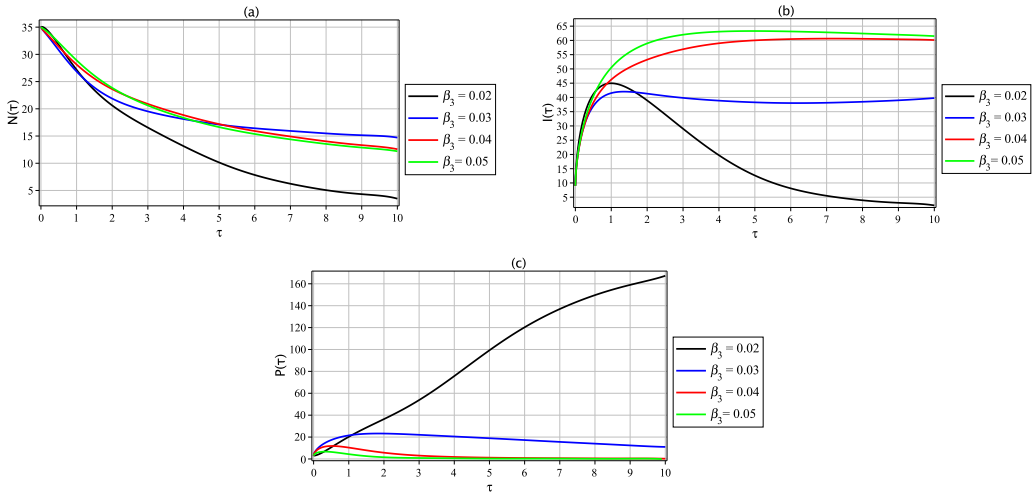

Fig. 6.14. Plots of approximate solutions to model (1.1): (a) $\mathcal{N}(\tau)$, (b) $\mathcal{I}(\tau)$, (c) $\mathcal{P}(\tau)$ for different values of β_3, $\zeta = 0.6$, $(\theta, \vartheta) = (1, 1)$, and $M = 7$.

where $U_i, i = 1, 2, 3$ are $(M + 1) \times 1$ vectors which must be determined. Now, suppose $\tau_j, j = 0, 1, \ldots, M$ are the roots of $\mathsf{J}_{M+1}^{(\theta,\vartheta)}(\tau)$. Approximations (6.1), (6.2), and (6.7) are substituted into (6.5) and (6.6), then the Lagrange multipliers method is applied to find appropriate values of state and control functions as follows:

$$\begin{aligned}\mathcal{F}_M = \int_0^{\top} \Big(& \eta_1 \left(\mathcal{N}_0 + \tau^{\zeta}\, \mathsf{C}_1^{\top} \Lambda^{(\zeta,\theta,\vartheta)}\, \mathbb{J}^{(\theta,\vartheta)}(\tau) \right) - \eta_2 \left(\mathcal{I}_0 + \tau^{\zeta}\, \mathsf{C}_2^{\top} \Lambda^{(\zeta,\theta,\vartheta)}\, \mathbb{J}^{(\theta,\vartheta)}(\tau) \right) \\ & + \eta_3 \left(\mathcal{P}_0 + \tau^{\zeta}\, \mathsf{C}_3^{\top} \Lambda^{(\zeta,\theta,\vartheta)}\, \mathbb{J}^{(\theta,\vartheta)}(\tau) \right) + \epsilon_1 \left(U_1^{\top} \mathbb{J}^{(\theta,\vartheta)}(\tau) \right)^2 + \epsilon_2 \left(U_2^{\top} \mathbb{J}^{(\theta,\vartheta)}(\tau) \right)^2 \\ & + \epsilon_3 \left(U_3^{\top} \mathbb{J}^{(\theta,\vartheta)}(\tau) \right)^2 \Big)\, d\tau + \Psi_1^{\top} \mathcal{R}_1^* + \Psi_2^{\top} \mathcal{R}_2^* + \Psi_3^{\top} \mathcal{R}_3^*, \end{aligned} \tag{6.8}$$

where $\Psi_i, \mathcal{R}_i^*, i = 1, 2, 3$ are the following vectors:

$$\begin{aligned} \Psi_i &= [\psi_i^0, \psi_i^1, \dots, \psi_i^M]^\top, && i = 1, 2, 3, \\ \mathcal{R}_i^* &= [\mathcal{W}_i(\tau_0), \mathcal{W}_i(\tau_1), \dots, \mathcal{W}_i(\tau_M)]^\top, && i = 1, 2, 3, \end{aligned}$$

where $\psi_i^j, i = 1, 2, 3, j = 0, 1, \dots, M$ are Lagrange multipliers and $\mathcal{W}_i(\tau), i = 1, 2, 3$ are the following approximate equations:

$$\begin{aligned} \mathcal{W}_1(\tau) &= \mathsf{C}_1^\top \mathbb{J}^{(\theta,\vartheta)}(\tau) - \lambda \left(\mathcal{N}_0 + \tau^\zeta \, \mathsf{C}_1^\top \Lambda^{(\zeta,\theta,\vartheta)} \, \mathbb{J}^{(\theta,\vartheta)}(\tau)\right) \left(1 - \frac{1}{\kappa}\left(\mathcal{N}_0 + \tau^\zeta \, \mathsf{C}_1^\top \Lambda^{(\zeta,\theta,\vartheta)} \, \mathbb{J}^{(\theta,\vartheta)}(\tau)\right)\right) \\ &\quad + \mu\left(\mathcal{N}_0 + \tau^\zeta \, \mathsf{C}_1^\top \Lambda^{(\zeta,\theta,\vartheta)} \, \mathbb{J}^{(\theta,\vartheta)}(\tau)\right)\left(\mathcal{P}_0 + \tau^\zeta \, \mathsf{C}_3^\top \Lambda^{(\zeta,\theta,\vartheta)} \, \mathbb{J}^{(\theta,\vartheta)}(\tau)\right) \\ &\quad + \beta_1\left(\mathcal{N}_0 + \tau^\zeta \, \mathsf{C}_1^\top \Lambda^{(\zeta,\theta,\vartheta)} \, \mathbb{J}^{(\theta,\vartheta)}(\tau)\right)\left(\mathcal{I}_0 + \tau^\zeta \, \mathsf{C}_2^\top \Lambda^{(\zeta,\theta,\vartheta)} \, \mathbb{J}^{(\theta,\vartheta)}(\tau)\right) \\ &\quad + \xi_1\left(U_1^\top \mathbb{J}^{(\theta,\vartheta)}(\tau)\right)\left(\mathcal{N}_0 + \tau^\zeta \, \mathsf{C}_1^\top \Lambda^{(\zeta,\theta,\vartheta)} \, \mathbb{J}^{(\theta,\vartheta)}(\tau)\right), \\ \mathcal{W}_2(\tau) &= \mathsf{C}_2^\top \mathbb{J}^{(\theta,\vartheta)}(\tau) - \varphi_1 \, \mathcal{I}_0 - \varphi_2\left(\mathcal{N}_0 + \tau^\zeta \, \mathsf{C}_1^\top \Lambda^{(\zeta,\theta,\vartheta)} \, \mathbb{J}^{(\theta,\vartheta)}(\tau)\right)^2 \\ &\quad + \varphi_3\left(\mathcal{I}_0 + \tau^\zeta \, \mathsf{C}_2^\top \Lambda^{(\zeta,\theta,\vartheta)} \, \mathbb{J}^{(\theta,\vartheta)}(\tau)\right) \\ &\quad + \beta_2\left(\mathcal{I}_0 + \tau^\zeta \, \mathsf{C}_2^\top \Lambda^{(\zeta,\theta,\vartheta)} \, \mathbb{J}^{(\theta,\vartheta)}(\tau)\right)\left(\mathcal{P}_0 + \tau^\zeta \, \mathsf{C}_3^\top \Lambda^{(\zeta,\theta,\vartheta)} \, \mathbb{J}^{(\theta,\vartheta)}(\tau)\right) \\ &\quad - \xi_2\left(U_2^\top \mathbb{J}^{(\theta,\vartheta)}(\tau)\right)\left(\mathcal{I}_0 + \tau^\zeta \, \mathsf{C}_2^\top \Lambda^{(\zeta,\theta,\vartheta)} \, \mathbb{J}^{(\theta,\vartheta)}(\tau)\right), \\ \mathcal{W}_3(\tau) &= \mathsf{C}_3^\top \mathbb{J}^{(\theta,\vartheta)}(\tau) - \gamma\left(\mathcal{N}_0 + \tau^\zeta \, \mathsf{C}_1^\top \Lambda^{(\zeta,\theta,\vartheta)} \, \mathbb{J}^{(\theta,\vartheta)}(\tau)\right)\left(\mathcal{P}_0 + \tau^\zeta \, \mathsf{C}_3^\top \Lambda^{(\zeta,\theta,\vartheta)} \, \mathbb{J}^{(\theta,\vartheta)}(\tau)\right) \\ &\quad + \delta\left(\mathcal{P}_0 + \tau^\zeta \, \mathsf{C}_3^\top \Lambda^{(\zeta,\theta,\vartheta)} \, \mathbb{J}^{(\theta,\vartheta)}(\tau)\right) \\ &\quad + \beta_3\left(\mathcal{I}_0 + \tau^\zeta \, \mathsf{C}_2^\top \Lambda^{(\zeta,\theta,\vartheta)} \, \mathbb{J}^{(\theta,\vartheta)}(\tau)\right)\left(\mathcal{P}_0 + \tau^\zeta \, \mathsf{C}_3^\top \Lambda^{(\zeta,\theta,\vartheta)} \, \mathbb{J}^{(\theta,\vartheta)}(\tau)\right) \\ &\quad + \xi_3\left(U_3^\top \mathbb{J}^{(\theta,\vartheta)}(\tau)\right)\left(\mathcal{P}_0 + \tau^\zeta \, \mathsf{C}_3^\top \Lambda^{(\zeta,\theta,\vartheta)} \, \mathbb{J}^{(\theta,\vartheta)}(\tau)\right). \end{aligned}$$

Eq. (6.8) involves $9(M+1)$ unknown coefficients $(\mathsf{C}_i^j, U_i^j, \Psi_i^j, i = 1, 2, 3, j = 0, 1, \dots, M)$ which must be determined. According to the method of Lagrange multipliers, the following nonlinear system involving $9(M+1)$ algebraic equations is achieved to calculate the solutions to problem (6.5)-(6.6):

$$\frac{\partial \mathcal{F}_M}{\partial \mathsf{C}_i} = 0, \quad \frac{\partial \mathcal{F}_M}{\partial U_i} = 0, \quad \frac{\partial \mathcal{F}_M}{\partial \Psi_i} = 0, \quad i = 1, 2, 3. \tag{6.9}$$

By solving system (6.9) by an iterative method, for instance, Newton's iteration method, unknown coefficients are estimated approximately, therefore approximate solutions to problem (6.5)-(6.6) are acquired.

Values of parameters, coefficients, and initial conditions of problem (6.5)-(6.6) are considered as follows [4]:

$$\begin{array}{lllllll} \lambda = 0.3, & \kappa = 10000, & \mu = 0.01, & \beta_1 = 0.0155, & \beta_2 = 0.03, & \beta_3 = 0.04, & \\ \phi_1 = 0.5, & \phi_2 = 0.3, & \phi_3 = 0.4, & \gamma = 0.07, & \delta = 0.001, & \eta_1 = 10, & \\ \eta_2 = 1, & \eta_3 = 10, & \epsilon_1 = 150, & \epsilon_2 = 100, & \epsilon_3 = 150, & \xi_1 = 0.08, & \\ \xi_2 = 0.05, & \xi_3 = 0.04, & \mathcal{N}_0 = 35, & \mathcal{I}_0 = 9, & \mathcal{P}_0 = 3, & M = 7, & T = 10. \end{array}$$

Plots of state variables $\mathcal{N}(\tau), \mathcal{I}(\tau)$, and $\mathcal{P}(\tau)$ are seen in Fig. 6.15 for $(\theta, \vartheta) = (0, 0), M = 7$, $\zeta = 0.1, 0.2, 0.3, 0.4, 0.5$. The number of cancer cells and cancer cells spread in other parts of the body are reduced by increasing values of ζ. In Fig. 6.15(b), the number of immune cells decreases by increasing values of ζ, but results are more desirable compared to curves in Fig. 6.5(b). In

Fig. 6.15(b), $\mathcal{I}(\tau)$ increases on $[0, 0.5]$ while $\mathcal{P}(\tau)$ decreases over this interval. $\mathcal{I}(\tau)$ decreases over $[0.5, 1]$ and all curves are almost constant after $\tau = 1$. The same behaviour is seen in Fig. 6.15(c). Plots of control variables $u_i(\tau), i = 1, 2, 3$ are depicted in Fig. 6.16 for $(\theta, \vartheta) = (0, 0), M = 7, \zeta = 0.1, 0.2, 0.3, 0.4, 0.5$. From Fig. 6.16(a) and (b), the cost of decreasing the number of cancer cells and increasing immune cells increases by increasing values of ζ, while the cost decreases after $\tau = 9$ in Fig. 6.16(b). However, the cost of decreasing the number of spread cancer cells is reduced after $\tau = 1$ by changing values of ζ. Figs. 6.17 and 6.18 are depicted plots

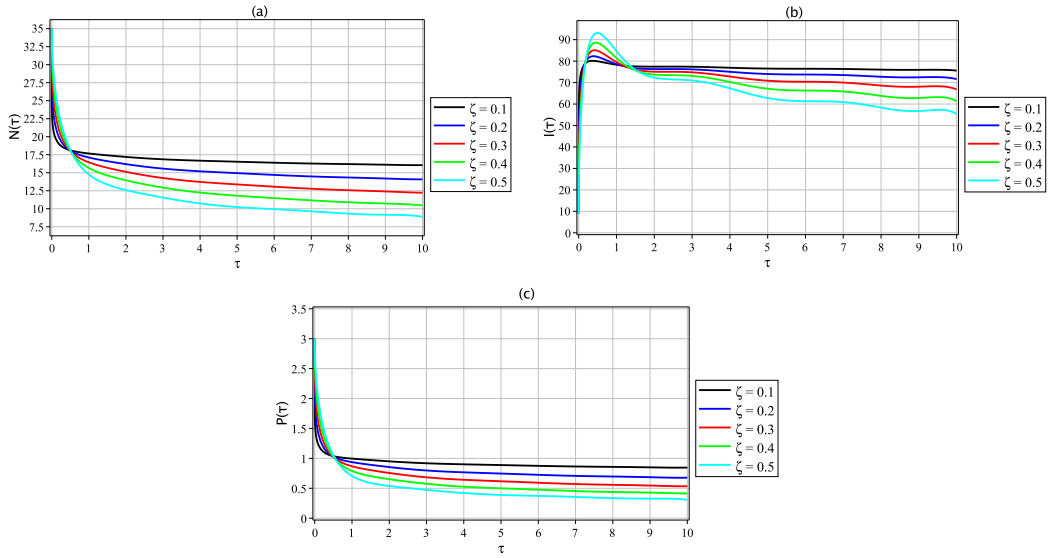

Fig. 6.15. Plots of control solutions to model (6.5): (a) $\mathcal{N}(\tau)$, (b) $\mathcal{I}(\tau)$, (c) $\mathcal{P}(\tau)$ for different values of ζ, $(\theta, \vartheta) = (0, 0)$, and $M = 7$.

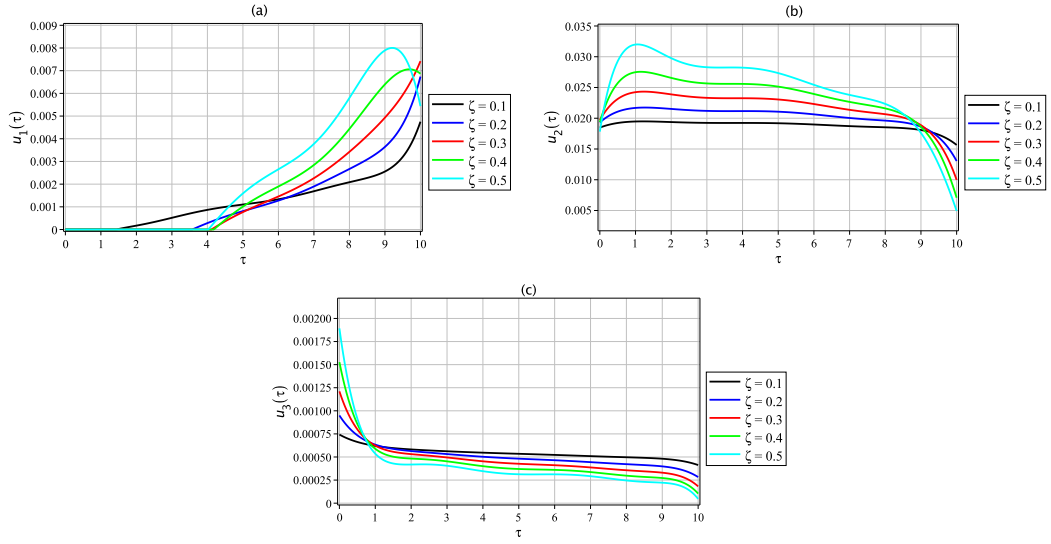

Fig. 6.16. Plots of control variables in model (6.5): (a) $u_1(\tau)$, (b) $u_2(\tau)$, (c) $u_3(\tau)$ for different values of ζ, $(\theta, \vartheta) = (0, 0)$, and $M = 7$.

of state and control functions, respectively, for $M = 7, (\theta, \vartheta) = (1, 1), \zeta = 0.1, 0.2, 0.3, 0.4, 0.5$. The figures have the same treatment of figures in 6.15 and 6.16, but $u_3(\tau)$ shows an oscillatory behaviour. Figures of state and control variables are observed in Figs. 6.19 and 6.20, respectively for $M = 7, (\theta, \vartheta) = (0.5, 0.5)$, and different values of ζ. Figures of state variables and control variables are seen in Figs. 6.21 and 6.22, respectively, for $M = 7, (\theta, \vartheta) = (-0.4, -0.25)$, and different values of ζ.

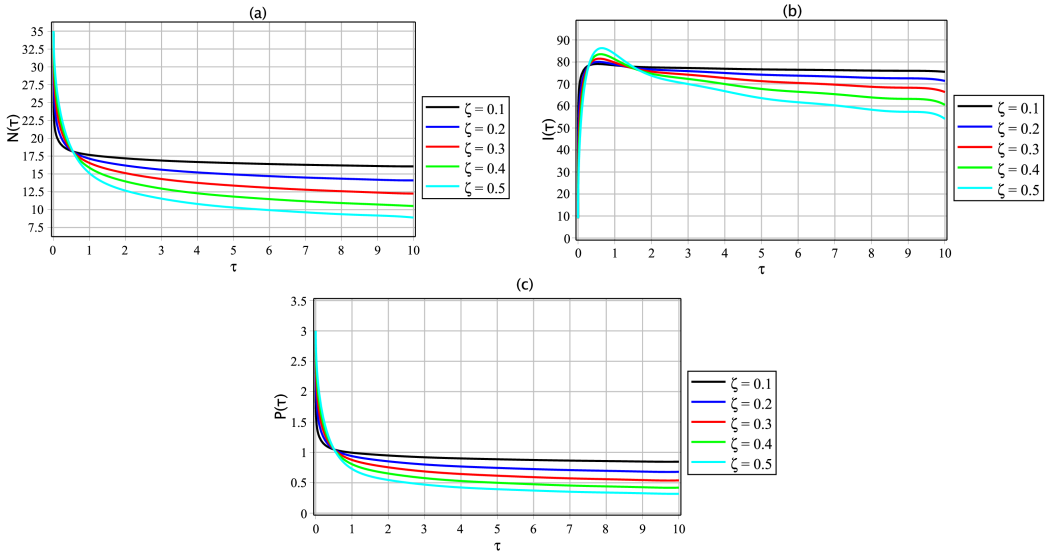

Fig. 6.17. Plots of control solutions to model (6.5): (a) $\mathcal{N}(\tau)$, (b) $\mathcal{I}(\tau)$, (c) $\mathcal{P}(\tau)$ for different values of ζ, $(\theta, \vartheta) = (1, 1)$, and $M = 7$.

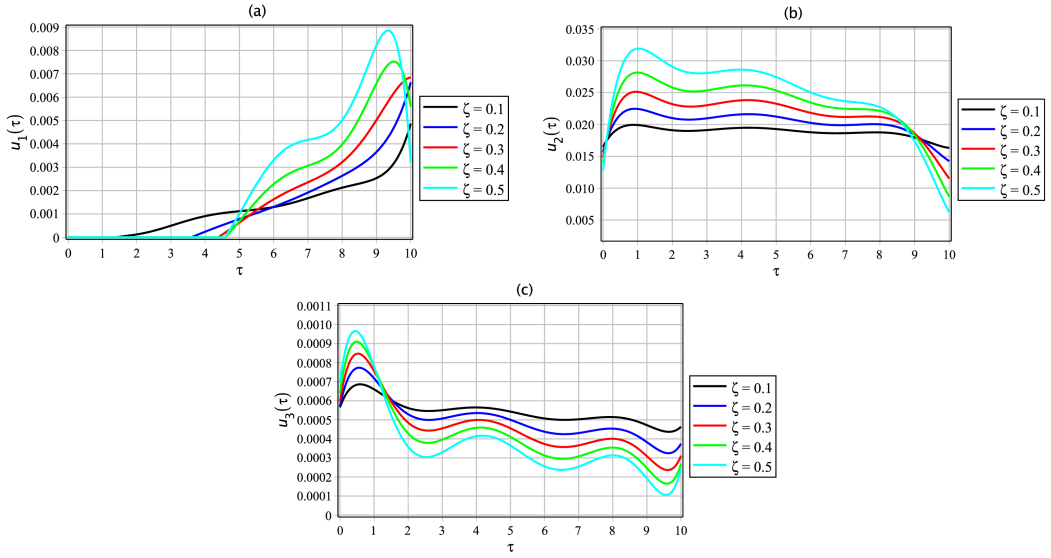

Fig. 6.18. Plots of control variables in model (6.5): (a) $u_1(\tau)$, (b) $u_2(\tau)$, (c) $u_3(\tau)$ for different values of ζ, $(\theta, \vartheta) = (1, 1)$, and $M = 7$.

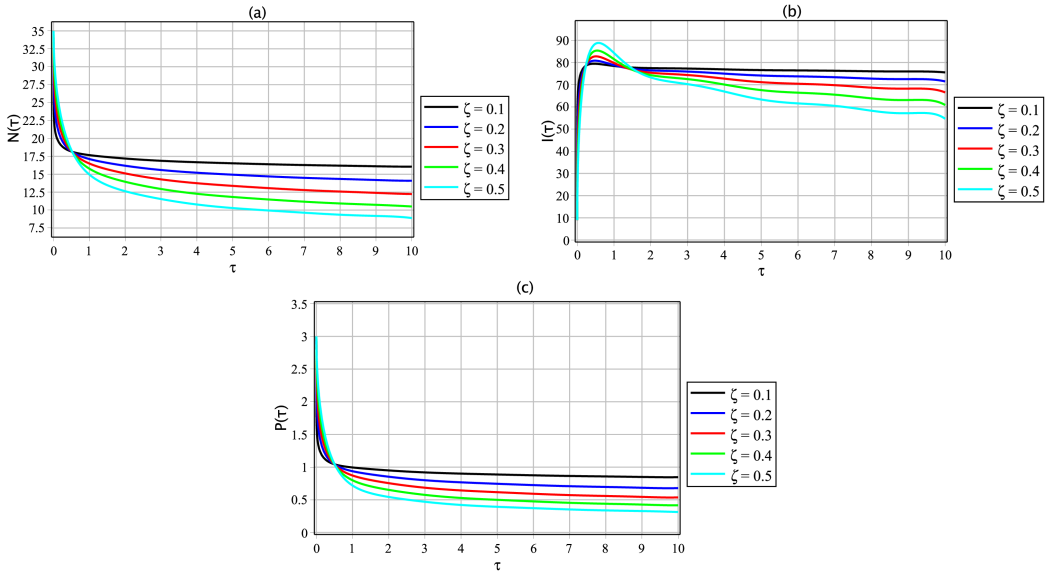

Fig. 6.19. Plots of control solutions to model (6.5): (a) $\mathcal{N}(\tau)$, (b) $\mathcal{I}(\tau)$, (c) $\mathcal{P}(\tau)$ for different values of ζ, $(\theta, \vartheta) = (0.5, 0.5)$, and $M = 7$.

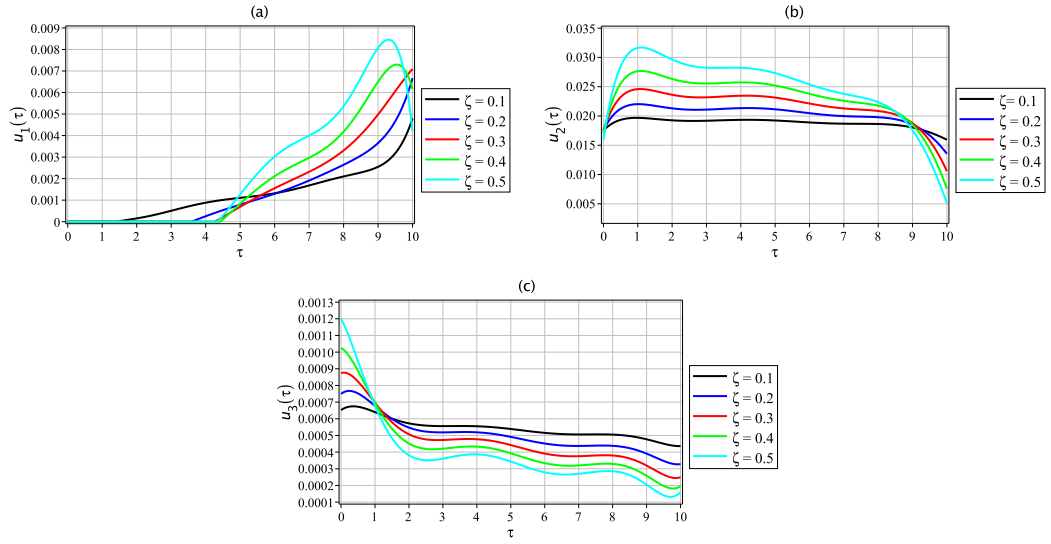

Fig. 6.20. Plots of control variables in model (6.5): (a) $u_1(\tau)$, (b) $u_2(\tau)$, (c) $u_3(\tau)$ for different values of ζ, $(\theta, \vartheta) = (0.5, 0.5)$, and $M = 7$.

7. Biological Interpretations of the Results

In a medical context, the fractional derivative order (ζ) represents a more comprehensive and memory-inclusive way to model biological processes. Unlike traditional integer-order derivatives that assume instantaneous rates of change, fractional derivatives account for the history of the system's states, providing a more accurate depiction of long-term interactions and dependencies. This approach acknowledges that current states and changes in cell populations are not

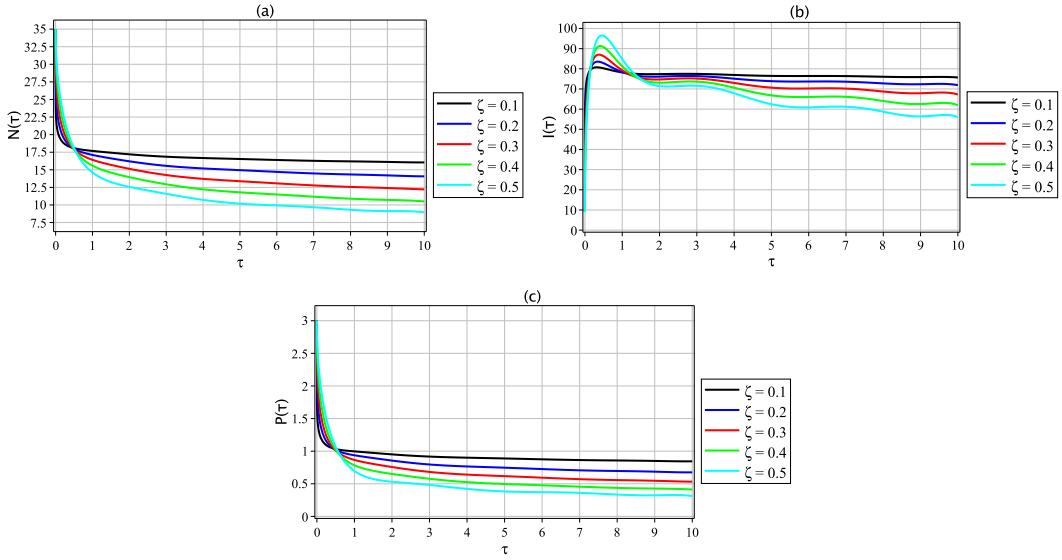

Fig. 6.21. Plots of control solutions to model (6.5): (a) $\mathcal{N}(\tau)$, (b) $\mathcal{I}(\tau)$, (c) $\mathcal{P}(\tau)$ for different values of ζ, $(\theta, \vartheta) = (-0.4, -0.25)$, and $M = 7$.

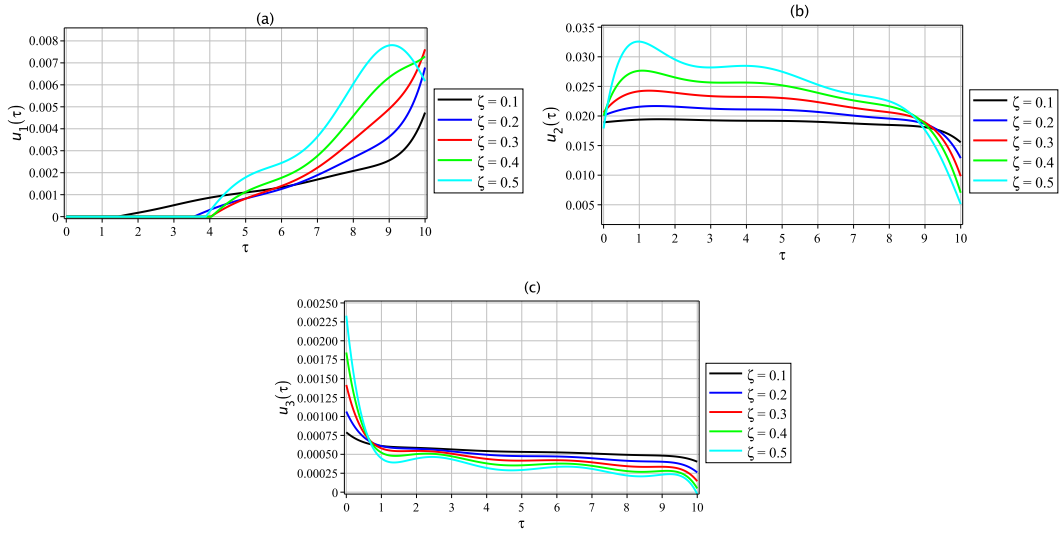

Fig. 6.22. Plots of control variables in model (6.5): (a) $u_1(\tau)$, (b) $u_2(\tau)$, (c) $u_3(\tau)$ for different values of ζ, $(\theta, \vartheta) = (-0.4, -0.25)$, and $M = 7$.

just dependent on immediate past conditions but also a broader range of past states. As ζ increases, the number of cancer cells ($\mathcal{N}(\tau)$) decreases, indicating that higher ζ values slow the growth of cancer cells. Concurrently, the number of immune cells ($\mathcal{I}(\tau)$) increases and stabilizes at approximately 60 after $\tau = 6$, suggesting that immune response improves with higher ζ. The metastatic cancer cells ($\mathcal{P}(\tau)$) initially increase but decrease significantly after $\tau = 0.5$, stabilizing at lower values. This indicates that increasing ζ effectively controls both local tumor growth and metastasis. Higher values of λ lead to a decrease in cancer cell populations, demonstrating

that modulating the growth rate can be an effective strategy in cancer control. Immune cell populations increase with λ up to $\tau = 0.5$, after which they decrease. This suggests a dynamic interaction where an initial rapid immune response might be followed by a reduction due to resource depletion or regulatory mechanisms. The propagation rate of cancer increases with λ, but eventually, all curves converge, indicating a common long-term behavior irrespective of λ. Increasing the interaction coefficient μ reduces cancer cell numbers, highlighting the importance of targeting cancer-immune interactions in therapy. However, higher μ reduces immune cell counts, indicating a possible trade-off between tumor suppression and immune cell viability. Higher values of β_1 reduce cancer cells but also significantly decrease immune cells, suggesting that while direct immune-mediated cancer cell killing is effective, it can be detrimental to immune cell populations if overactivated. Conversely, increasing β_2 leads to increased cancer cell numbers and propagation rates, making it a less favorable strategy for controlling cancer spread. The parameters φ_1 and φ_3 show minimal impact on the state variables, indicating that these parameters might not be critical in this context or that their roles are more complex and require further investigation. Increasing φ_2 generally improves immune response and reduces cancer cell numbers, underscoring the potential benefits of enhancing immune activation mechanisms. However, undesirable results for lower φ_2 suggest that there is a threshold above which immune enhancement becomes effective. Higher γ values increase the spread of cancer to other parts of the body and decrease immune cell counts, indicating that controlling metastatic potential is crucial for effective cancer management. Increasing δ reduces metastatic cancer cell numbers, suggesting that enhancing cancer cell death rates could be a beneficial strategy in controlling metastasis. Higher values of β_3 (except for $\beta_3 = 0.02$) decrease both primary and metastatic cancer cells while increasing immune cells, indicating that modulating this parameter could provide a balanced approach to reducing tumor burden and supporting immune function.

Figs. 6.15(a)-(c) show the control solutions for the state variables $\mathcal{N}(\tau), \mathcal{I}(\tau)$, and $\mathcal{P}(\tau)$ for $(\theta, \vartheta) = (0, 0), M = 7$, and $\zeta = 0.1, 0.2, 0.3, 0.4, 0.5$. Increasing values of ζ lead to a reduction in the number of cancer cells in the lung tissues, indicating that higher fractional derivative orders, which account for the historical behavior of the system, are effective in controlling tumor growth. Although the number of immune cells decreases with increasing ζ, the results are more favorable compared to those without feedback control strategy (Fig. 6.5(b)). This suggests that while the immune response might be initially suppressed, the overall effect is beneficial in reducing tumor burden. The number of metastatic cancer cells decreases with increasing ζ, showing that higher fractional orders help in controlling the spread of cancer to other parts of the body. In Fig. 6.15(b), $\mathcal{I}(\tau)$ increases over $[0, 0.5]$ while $\mathcal{P}(\tau)$ decreases, suggesting an initial boost in the immune response that curtails metastasis. After $\tau = 0.5, \mathcal{I}(\tau)$ decreases, and the state variables stabilize after $\tau = 1$, indicating a steady-state response. Figs. 6.16(a)-(c) show the control variables $u_i(\tau), i = 1, 2, 3$, for $(\theta, \vartheta) = (0, 0), M = 7$, and $\zeta = 0.1, 0.2, 0.3, 0.4, 0.5$. The cost of decreasing the number of cancer cells and increasing immune cells increases with higher ζ, but the cost decreases after $\tau = 9$ (Fig. 6.16(b)). This suggests that initial intervention costs might be high but stabilize over time. The cost of reducing metastatic cancer cells decreases after $\tau = 1$ with varying ζ, indicating that early intervention is crucial and becomes more efficient as time progresses. Figs. 6.17 and 6.18 depict controlled state and control functions for $M = 7, (\theta, \vartheta) = (1, 1)$, and $\zeta = 0.1, 0.2, 0.3, 0.4, 0.5$. These figures show similar trends as observed previously, with $u_3(\tau)$ exhibiting an oscillatory behavior, suggesting a dynamic adjustment in the control strategy. Figs. 6.19 and 6.20 display the controlled state variables and control variables for $M = 7, (\theta, \vartheta) = (0.5, 0.5)$, and different values of ζ. These figures confirm

that varying ζ continues to influence the effectiveness of the control strategies. Figs. 6.21 and 6.22 present controlled state variables and control variables for $M = 7, (\theta, \vartheta) = (-0.4, -0.25)$, and different values of ζ. The trends remain consistent, emphasizing the robustness of the feedback control approach across different parameter settings. The control solutions derived from the fractional-order mathematical model provide critical insights into the effective management of lung cancer. By incorporating the historical behavior of the system through fractional derivatives, the model offers a sophisticated approach to controlling tumor growth and metastasis. The results highlight the importance of early and sustained intervention, as well as the potential trade-offs between immediate costs and long-term benefits. These findings can inform the development of more targeted and efficient therapeutic strategies in clinical settings.

8. Conclusion

A pseudo-operational collocation approach based on shifted Jacobi polynomials was proposed to seek spectral solutions of a mathematical model of the growth of cancer in the lung tissues over the interval $[0, T], T > 1$. The existence and uniqueness of solutions to the given model were proven by employing Leray-Schauder fixed point theorem before going to the numerical solution. The integral pseudo-operational matrix of the fractional order ζ was constructed by some algebraic manipulation on the basis vector. Some error bounds were estimated in a Jacobi-weighted L^2-space, then by utilizing obtained bounds, error bounds of residual functions showed that if the number of basis functions is large enough, then the upper bounds can be small enough. Using resultant approximations to the given model led to approximate solutions which drawing approximate solutions demonstrated the dynamic of the model and the behaviour of the state functions. In all results, the number of cancer cells and the number of spread cancer cells in other parts of the body decreased, while the number of immune cells increased by increasing values of the fractional order ζ. Shifted Jacobi polynomials were considered with different values of parameters θ and ϑ and the effect of changing values of parameters has been seen on $\mathcal{P}(\tau)$. In order to improve the efficiency of outputs, two different strategies were adopted: sensitivity analysis and feedback control. Increasing values of parameters like λ, γ, and β_2 led to increase the number of cancer cells and the propagation of cancer cells in other parts of the body. Besides with the increase of values of parameters like μ, β_1, and δ, the number of cancer cells decreases in lung tissues. Decreasing values of φ_2 or β_3 are not recommended. In the feedback control section, the target was to decrease the number of cancer cells and increase the number of immune cells. This target was pursued by inputting three control functions. To determine appropriate values of control functions with the target of minimizing the objective function, the method of Lagrange multipliers has been applied. This application resulted in a non-linear system involving $9(M + 1)$ algebraic equations. Solving the resultant system led to desired approximate solutions to model (6.5). Plotting obtained solutions related to the feedback control strategy showed the better treatment of outputs.

Authors in [20, 32] introduced a weighted-Jacobi polynomials for two-sided fractional diffusion equations to increase the convergence rate. As a future plan, authors will use this idea to solve 2D time-fractional diffusion-wave equations to reduce the approximation error.

Acknowledgements. We are very grateful to anonymous referees for their careful reading and valuable comments, which led to the improvement of this paper.

References

[1] C. Abbosh, D. Hodgson, G.J. Doherty, D. Gale, J.R.M. Black, L. Horn, J.S. Reis-Filho, and C. Swanton, Implementing circulating tumor DNA as a prognostic biomarker in resectable non-small cell lung cancer, *Trends Cancer*, **10**:7 (2024), 643–654.

[2] M.A. Abdelkawy, A.M. Lopes, and M.M. Babatin, Shifted fractional Jacobi collocation method for solving fractional functional differential equations of variable order, *Chaos Solitons Fractals*, **134** (2020), 109721.

[3] W.M. Ahmad and R. El-Khazali, Fractional-order dynamical models of love, *Chaos Solitons Fractals*, **33** (2007), 1367–1375.

[4] D. Amilo, B. Kaymakamzade, and E. Hincal, A fractional-order mathematical model for lung cancer incorporating integrated therapeutic approaches, *Sci. Rep.*, **13** (2023), 12426.

[5] D. Amilo, K. Sadri, B. Kaymakamzade, and E. Hincal, A mathematical model with fractional-order dynamics for the combined treatment of metastatic colorectal cancer, *Commun. Nonlinear Sci. Numer. Simul.*, **130** (2024), 107756.

[6] A. Atmakuru, S. Chakraborty, O. Faust, M. Salvi, P.D. Barua, F. Molinari, U.R. Acharya, and N. Homaira, Deep learning in radiology for lung cancer diagnostics: A systematic review of classification, segmentation, and predictive modeling techniques, *Expert Syst. Appl.*, **255** (2024), 124665.

[7] Attaullah and M. Sohaib, Mathematical modeling and numerical simulation of HIV infection model, *Results Appl. Math.*, **7** (2020), 100118.

[8] Z. Avazzadeh, H. Hassani, P. Agarwal, S. Mehrabi, M.J. Ebadi, and M.S. Dahaghin, An optimization method for studying fractional-order tuberculosis disease model via generalized Laguerre polynomials, *Soft Comput.* **27** (2023), 9519–9531.

[9] Z. Avazzadeh, H. Hassani, M.J. Ebadi, A.B. Eshkaftaki, R. Katani, and A. Rezvani, Generalization of Bernoulli polynomials to find optimal solution of fractional hematopoietic stem cells model, *Phys. Scr.* **99** (2024), 085015.

[10] T.K. Ayele, E.F.D. Goufo, and S. Mugisha, Mathematical modeling of HIV/AIDS with optimal control: A case study in Ethiopia, *Results Phys.* **26** (2021), 104263.

[11] W. Banzi, I. Kambutse, V. Dusabejambo, E. Rutaganda, F. Minani, J. Niyobuhungiro, L. Mpinganzima, and J.M. Ntaganda, Mathematical modelling of glucose-insulin system and test of abnormalities of type 2 diabetic patients, *Int. J. Math. math. Sci.*, **2021** 2021, 6660177.

[12] A.H. Bhrawy, M.M. Tharwat, and A. Yildirim, A new formula for fractional integrals of Chebyshev polynomials: Application for solving multi-term fractional differential equations, *Appl. Math. Model.*, **37** (2013), 4245–4252.

[13] Z. Chen, I.H.M. Wong, W. Dai, C.T.K. Lo, and T.T.W. Wong, Lung cancer diagnosis on virtual histologically stained tissue using weakly supervised learning *Mod. Pathol.*, **37**:6 (2024), 100487.

[14] M. Dehghan and F. Fakhar-Izadi, The spectral collocation method with three different bases for solving a nonlinear partial differential equation arising in modeling of nonlinear waves, *Math. Comput. Model.*, **53** (2011), 1865–1877.

[15] A.D.F. Diethelm, On the solution of nonlinear fractional-order differential equations used in the modeling of viscoplasticity, in: *Scientific Computing in Chemical Engineering II: Computational Fluid Dynamics, Reaction Engineering, and Molecular Properties*, Springer, (1999), 217–224.

[16] E.H. Doha, A.H. Bhrawy, and S.S. Ezz-Eldien, A new Jacobi operational matrix: An application for solving fractional differential equations, *Appl. Math. Model.*, **36** (2012), 4931–4943.

[17] E.H. Doha, R.M. Hafez, and Y.H. Youssri, Shifted Jacobi spectral-Galerkin method for solving hyperbolic partial differential equations, *Comput. Math. Appl.*, **78**:3 (2019), 889–904.

[18] R.M. Ganji, H. Jafari, S.P. Moshokoa, and N.S. Nkomo, A mathematical model and numerical solution for brain tumor derived using fractional operator, *Results Phys.*, **28** (2021), 104671.

[19] W. Gautschi, *Orthogonal Polynomials: Computation and Approximation*, Oxford University

Press, 2004.
[20] Z.P. Hao, G. Lin, and Z. Zhang, Regularity and spectral methods for two-sided fractional diffusion equations with a low-order term, *arXiv.1705.07209*, 2017.
[21] H. Hassani, Z. Avazzadeh, P. Agarwal, S. Mehrabi, M.J. Ebadi, M.S. Dahaghin, and E. Naraghirad, A study on fractional tumor-immune interaction model related to lung cancer via generalized Laguerre polynomials, *BMC Med. Res. Methodol.*, **23** (2023), 189.
[22] M.H. Heydari, M. Razzaghi, and D. Baleanu, A numerical method based on the piecewise Jacobi functions for distributed-order fractional Schrodinger equation, *Commun. Nonlinear Sci. Numer. Simul.*, **116** (2023), 106873.
[23] M.H. Heydari, Sh. Zhagharian, and M. Razzaghi, Jacobi polynomials for the numerical solution of multi-dimensional stochastic multi-order time fractional diffusion-wave equations, *Comput. Math. Appl.*, **152** (2023), 91–101.
[24] M. Hosseininia, M.H. Heydari, and Z. Avazzadeh, Orthonormal shifted discrete Legendre polynomials for the variable-order fractional extended Fisher-Kolmogorov equation, *Chaos Solitons Fractals*, **155** (2022), 111729.
[25] T. Kanwal, A. Hussain, I. Avci, S. Etemad, S. Rezapour, and D.F.M. Torres, Dynamics of a model of polluted lakes via fractal-fractional operators with two different numerical algorithms, *Chaos Solitons Fractals*, **181** (2024), 114653.
[26] Y. Keskin, O. Karaoglu, S. Servi, and G. Oturan, The approximate solution of high order linear fractional differential equations with variable coefficients in terms of generalized Taylor series, *Math. Comput. Appl.*, **16** (2011), 617–629.
[27] M.M. Khader and N.H. Sweilam, On the approximate solutions for system of fractional integro-differential equations using Chebyshev pseudo-spectral method, *Appl. Math. Model.*, **37**:24 (2013), 9819–9828.
[28] A. Lahiri, A. Maji, P.D. Potdar, N. Singh, P. Parikh, B. Bisht, A. Mukherjee, and M.K. Paul, Lung cancer immunotherapy: Progress, pitfalls, and promises, *Mol. Cancer.* **22**:1 (2023), 40.
[29] X.J. Li and C.J. Xu, A space-time spectral method for the time fractional diffusion equation, *SIAM. J. Numer. Anal.*, **47**:3 (2009), 2108–2131.
[30] F. Mainardi, *Fractals and Fractional Calculus Continuum Mechanics*, Springer, (1997), 291–348.
[31] N. Maleki and S.T.A. Niaki, An intelligent algorithm for lung cancer diagnosis using extracted features from computerized tomography images, *Healthcare Anal.*, **3** (2023), 100150.
[32] Z. Mao and G.E. Karniadakis, A spectral method (of exponential convergence) for singular solutions of the diffusion equation with general two-sided fractional derivative, *SIAM J. Numer. Anal.*, **56**:1 (2018), 24–49.
[33] H.R. Marasi, M.H. Derakhshan, and A.A. Ghuraibawi, A novel method based on fractional order Gegenbauer wavelet operational matrix for the solutions of the multi-term time-fractional telegraph equation of distributed order, *Math. Comput. Simul.*, **217** (2024), 405–424.
[34] H.K. Matthews, C. Bertoli, and R.A.M. de Bruin, Cell cycle control in cancer, *Nat. Rev. Mol. Cell Biol.*, **23**:1 (2022), 74–88.
[35] P. Mokhtary, Discrete Galerkin method for fractional integro-differential equations, *Acta Math. Sci.*, **36B**:2 (2016), 560–578.
[36] B.J. Nath, K. Sadri, H.K. Sarmah, and K. Hosseini, An optimal combination of antiretroviral treatment an immunotherapy for controlling HIV infection, *Math. Comput. Simul.*, **217** (2024), 226–243.
[37] S. Nemati, Numerical solution of Volterra-Fredholm integral equations using Legendre collocation method, *J. Comput. Appl. Math.*, **278** (2015), 29–36.
[38] F. Ozkose, S. Ylmaz, M. Yavuz, I. Ozturk, M.T. Senel, B.S. Bagc, M. Dogan, and O. Onal, A fractional modeling of tumor-immune system interaction related to lung cancer with real data, *Eur. Phys. J. Plus.*, **137** (2022), 40.
[39] I. Podlubni, *Fractional Differential Equations*, Academic Press, 1999.

[40] K. Sadri, D. Amilo, K. Hosseini, E. Hincal, and A.R. Seadawy, A tau-Gegenbauer spectral approach for systems of fractional integro-differential equations with the error analysis, *AIMS Math.*, **9**:2 (2024), 3850–3880.

[41] H. Saeidi, M.S. Dahaghin, S. Mehrabi, and H. Hassani, An optimal solution for tumor growth model using generalized Bessel polynomials, *Math. Methods Appl. Sci.*, **48** (2025), 716–730.

[42] S. Seridevi and A. RajivKannan, Development of 3DTDUnet^{++} with novel function and multi-scale dilated-based deep learning model for lung cancer diagnosis using CT images, *Biomed. Signal Process. Control.*, **94** (2024), 106243.

[43] G. Szego, *Orthogonal Polynomials*, AMS, 1939.

[44] M.H. Tao, *Epidemiology of Lung Cancer. Lung Cancer and Imaging*, IOP Publishing Ltd, 2019.

[45] D. Varol Bayram and A. Dascoglu, A method for fractional Volterra integro-differential equations by Laguerre polynomials, *Adv. Differential Equations*, **2018** (2018), 466.

[46] X. Wang, D. Gu, J. Wei, H. Pan, L. Hou, M. Zhang, X. Wu, and H. Wang, Network evolution of core symptoms after lung cancer thoracoscopic surgery: A dynamic network analysis, *Eur. J. Oncol. Nurs.*, **70** (2024), 102546.

[47] S. Yaghoubi, H. Aminikhah, and K. Sadri, A new efficient method for solving systems of weakly singular fractional integro-differential equations by shifted sixth-kind Chebyshev polynomials, *J. Math.*, **2022** (2022), 9087359.

[48] S. Yaghoubi, H. Aminikhah, and K. Sadri, A spectral shifted Gegenbauer collocation method for fractional pantograph partial differential equations and its error analysis, *Sadhana*, **48** (2023), 213.

[49] X. Yang, C. Wu, W. Wu, K. Fu, Y. Tian, X. Wei, W. Zhang, P. Sun, H. Luo, and H. Huang, A clinical-information-free method for early diagnosis of lung cancer from the patients with pulmonary nodules based on backpropagation neural network model, *Comput. Struct. Biotechnol. J.*, **24** (2024), 404–411.

[50] Y. Yang, Convergence analysis of the Jacobi spectral-collocation method for fractional integro-differential equations, *Acta Math. Sci.*, **34B**:3 (2014), 673–690.

[51] Y.H. Youssri and A.G. Atta, Spectral collocation approach via normalized shifted Jacobi polynomials for the nonlinear Lane-Emden equation with fractal-fractional derivative, *Fractal Fract.*, **7** (2023), 133.